AD-A098 064 NAVAL POSTGRADUATE SCHOOL MONTEREY CA F/G 20/1
FINITE-AMPLITUDE STANDING WAVES IN A RECTANGULAR CAVITY WITH WE--ETC(U)
DEC 80 I JOUNG

UNCLASSIFIED NL

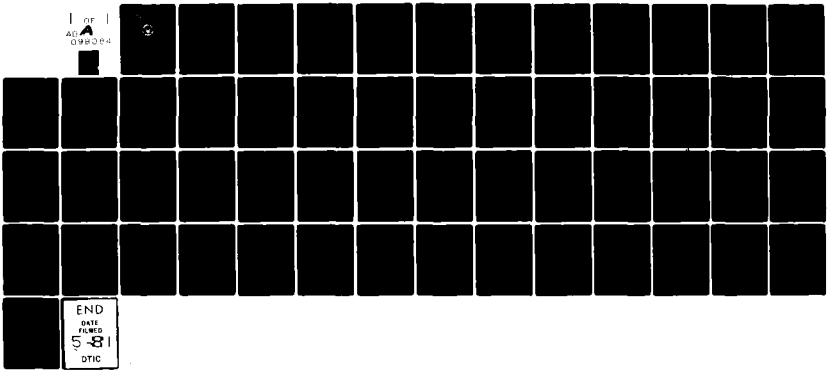

END
DATE FILMED
5-81
DTIC

NAVAL POSTGRADUATE SCHOOL
Monterey, California

THESIS

FINITE-AMPLITUDE STANDING WAVES IN A RECTANGULAR CAVITY WITH WEDGE-TYPE BOUNDARY PERTURBATION

by

Ilbok Joung

December 1980

Thesis Advisor: James V. Sanders

Unclassified

SECURITY CLASSIFICATION OF THIS PAGE (When Data Entered)

REPORT DOCUMENTATION PAGE		READ INSTRUCTIONS BEFORE COMPLETING FORM
1. REPORT NUMBER	2. GOVT ACCESSION NO. AD-A097864	3. RECIPIENT'S CATALOG NUMBER
4. TITLE (and Subtitle) Finite-Amplitude Standing Waves in a Rectangular Cavity With Wedge-Type Boundary Perturbation		5. TYPE OF REPORT & PERIOD COVERED Master's Thesis; December 1980
		6. PERFORMING ORG. REPORT NUMBER
7. AUTHOR(s) Ilbok Joung		8. CONTRACT OR GRANT NUMBER(s)
9. PERFORMING ORGANIZATION NAME AND ADDRESS Naval Postgraduate School Monterey, California 93940		10. PROGRAM ELEMENT, PROJECT, TASK AREA & WORK UNIT NUMBERS
11. CONTROLLING OFFICE NAME AND ADDRESS Naval Postgraduate School Monterey, California 93940		12. REPORT DATE December 1980
		13. NUMBER OF PAGES 54 pages
14. MONITORING AGENCY NAME & ADDRESS(if different from Controlling Office) Naval Postgraduate School Monterey, California 93940		15. SECURITY CLASS. (of this report) Unclassified
		15a. DECLASSIFICATION/DOWNGRADING SCHEDULE

16. DISTRIBUTION STATEMENT (of this Report)
Approved for public release; distribution unlimited

17. DISTRIBUTION STATEMENT (of the abstract entered in Block 20, if different from Report)

18. SUPPLEMENTARY NOTES

19. KEY WORDS (Continue on reverse side if necessary and identify by block number)
Finite amplitude standing waves

20. ABSTRACT (Continue on reverse side if necessary and identify by block number)

Finite amplitude acoustic standing waves in a rectangular air-filled cavity with various wedge-shape boundary perturbations were studied both experimentally and theoretically.

The experimental results showed that geometrical perturbations alter the finite amplitude behavior of the cavity and that the nature of these changes are in qualitative agreement with the predictions of the theory. However, quantitative agreement was not observed

DD FORM 1 JAN 73 1473 EDITION OF 1 NOV 65 IS OBSOLETE
S/N 0102-014-6601

(Page 1)

Unclassified

SECURITY CLASSIFICATION OF THIS PAGE (When Data Entered)

Item 20.

possibly because the perturbation chosen did not satisfy all the assumptions of theory.

There does not seem to be any fundamental obstacle preventing the choice of a perturbation that would allow the theory to be critically tested.

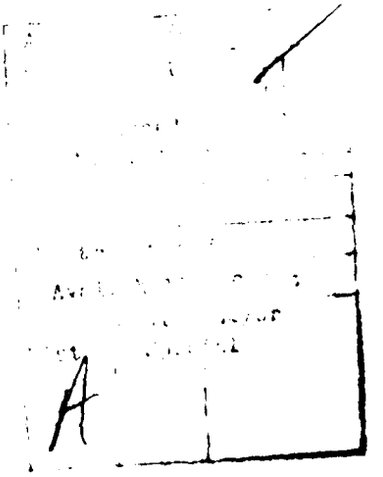

Approved for public release; distribution unlimited

Finite-Amplitude Standing Waves in a Rectangular Cavity With Wedge-Type Boundary Perturbation

by

Ilbok Joung
Lieutenant Commander, Korean Navy
B.S.E.E., Seoul National University, 1974

Submitted in partial fulfillment of the
requirements for the degree of

MASTER OF SCIENCE IN PHYSICS

from the

NAVAL POSTGRADUATE SCHOOL
December 1980

Author _____

Approved by: _____
Thesis Advisor

_____
Second Reader

_____
Chairman, Department of Physics and Chemistry

_____
Dean of Science and Engineering

ABSTRACT

Finite amplitude acoustic standing waves in a rectangular air-filled cavity with various wedge-shape boundary perturbations were studied both experimentally and theoretically.

The experimental results showed that geometrical perturbations alter the finite amplitude behavior of the cavity and that the nature of these changes are in qualitative agreement with the predictions of the theory. However, quantitative agreement was not observed possibly because the perturbation chosen did not satisfy all the assumptions of theory.

There does not seem to be any fundamental obstacle preventing the choice of a perturbation that would allow the theory to be critically tested.

TABLE OF CONTENTS

ACKNOWLEDGEMENT

The generous aid and encouragement of Professors James V. Sanders and Alan B. Coppens is gratefully acknowledged.

My sincere thanks to both professors and also to Mr. Bob Moller who provided several wedges.

I. INTRODUCTION

Coppens and Sanders [1,2] developed a non-linear acoustic model with the dissipative term describing the viscous and thermal energy losses encountered at the walls of a rectangular rigid cavity.

Several researchers [3,4] have examined the problems and experimental results are in excellent agreement with the theory except when a degeneracy exists in the cavity.

The purpose of this research was to examine the finite amplitude behavior at the cavity in the region for which perturbation effects can be accurately measured and to compare the results with the predictions of the model.

II. BACKGROUND AND THEORY

In 1975 [2] Coppens and Sanders formulated a perturbation expansion for the non-linear acoustic wave equation with a dissipative term describing the thermal energy loss and the non-ideal nature of cavity.

This model predicts that when a near-degeneracy exists, geometrical perturbations provide a mechanism whereby a nearly degenerate mode can affect the finite amplitude behavior of the cavity. (Most of the following theoretical developments were quoted from [2].)

The non-linear wave equation of the viscous fluid [2] is,

$$(C_o^2 \Box^2 + \frac{\partial}{\partial t}\mathcal{L}) \frac{P}{p_o C_o^2} = \frac{\partial^2}{\partial t^2} [(\frac{\mu}{C_o})^2 + \frac{8-1}{2} (\frac{P}{p_o C_o^2}) \quad (1)$$

where $\mathcal{L}$ is an operator describing the physical processes for absorption and dispersion. The right side term can be interpreted as a virtual source distributed within the cavity created by the finite-amplitude interaction of the linear waves.

The standing pressure wave in the rectangular cavity has the form

$$p \sim \cos k_x X \cos ky\ Y \cos k_z\ Z \cos wt$$

If the cavity is being driven near resonance, the non-resonant terms contribute almost nothing with respect

to the resonant terms. So the standing wave pressure has the form of

$$P = \sum_{n=1}^{\infty} p_n \tag{2}$$

where $\frac{P_n}{P_o C_o^2} = MR_n \cos nk_x X \cos nk_y Y \cox n k_z Z \sin (nwt + \phi_n)$

By substituting (2) into (1), a set of coupled, non-linear, transcendental are obtained;

$$R_n \begin{Bmatrix}\cos\\ \sin\end{Bmatrix} (\phi_n - \theta_n) = NM\beta Q_n \cos \theta_n \left[\tfrac{1}{2} \sum_{j=1}^{n-1} R_j R_{n-j} \begin{Bmatrix}\cos\\ \sin\end{Bmatrix} (\phi_j - \phi_{n-j}) - \sum_{j=1}^{\infty} R_{n+j} R_j \begin{Bmatrix}\cos\\ \sin\end{Bmatrix} (\phi_{n+j} - \phi_j)\right] \tag{3}$$

for all $n>1$, $N = \frac{1}{2^D}$

where D indicates the spatial dimension (D = 1, 2, 3).

If a geometrically perfect rectangular cavity is driven at frequencies near the resonance frequency of the (0,1,0) mode, $A_{oo} = 0$ and only the "family members" (o,n,o) will contribute to the finite amplitude behavior.

In this research we were interested in the behavior when a degeneracy exists between the 020 and 100 modes with small perturbations on the boundary. By using the boundary condition, $p \cdot n$ it can be shown that

$$P = p_{2w} + \varepsilon p' + \varepsilon^2 p'' + \ldots \approx p_{2w} + \varepsilon p' \tag{4}$$

where p_{2w} is the pressure of (0,2,0) mode, ε is the perturbation constant defined as the ratio of a geometric

perturbation magnitude (Δ) to the width (L_x) and p is (1,0,0) mode component.

Equation (4) can be expanded

$$p = p_{o2o} + \frac{2\varepsilon}{\left(\frac{2w}{C_o}\right)^2 L_x} A_{oo} S_{100} p_{100} e^{i(2wt + \theta + \tau_{oo})} \quad (5)$$

where $S_{100} \equiv Q_{100} \sin \tau_{100} x \frac{Q_{100}}{(1 + F_{100}^2)^{\frac{1}{2}}}$, A_{oo} is the first coefficient of the Fourier transform of the perturbation. Equation (5) describes how much energy of the (1,0,0) can be transferred to the (0,2,0) mode.

III. DEFINITION OF SOME PARAMETERS

Several parameters were defined for the purpose of simplifying the mathematical formulation without loss of physical contents.

A. STRENGTH PARAMETERS (STRM)

STRPM = MPQ_1 characterizes the strength of the finite-amplitude interaction. Since the microphone sensitivity (Sm obtained with B&K 4220 pistonphone) is known,

$$STRPM \equiv M\beta Q_1 = 7.07 \times 10^{-3} V_1 Q_1$$

where $M = \frac{\sqrt{2}\, V_1}{PC^2 S_M}$, $\beta = \frac{1}{2}(1 + \frac{C_p}{C_v}) = 1.2$ with $\frac{C_p}{C_v} = 1.4$

$P = 1.293\ Kg/m^3$, $C = 345\ m/sec$

V_1 = RMS output voltage of the first harmonic component

B. FREQUENCY PARAMETER (FP)

$$FP \equiv \frac{2Q_n(f-nf_1)}{nf_1}$$

where f is a resonant frequency of (0,1,0) mode, it is the driving frequency it is assumed that $\frac{\Delta w_n}{w_n} << 1$.

FP indicates where the driving frequency is with respect to the fundamental resonance frequency of the cavity. As |FP| increases, the non-linear effects become smaller.

C. HARMONICITY COEFFICIENT (E(n)

$$E(n) = \frac{f_n - nf_1}{nf_1} = \frac{FP_n}{2Q_n}$$

E(n) characterizes how well the modes of a given family are tuned. If E(n) <4|, the corresponding harmonic will be strongly excited.

IV. THE PRESSURE DISTRIBUTION WITH A WEDGED PERTURBATION

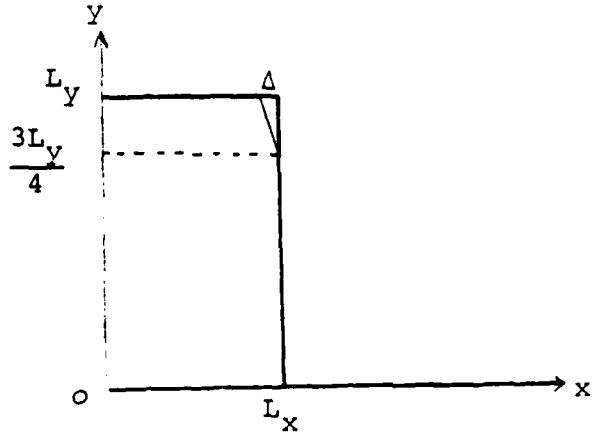

The pressure distribution of (0,2,0) mode has the form

$$P_{020} = P \cos \frac{2\pi}{L_y} y \cos (2wt + \theta_2) \tag{1}$$

The equation for the perturbed boundary is

$$X = L_x\{1- \frac{\Delta}{L_x} [\frac{4}{L_y} (y-\frac{3}{4}L_y)] [U (y-\frac{3L_y}{4}) - U (y-L_y)]\} \tag{2}$$

$$= L_x [1+\varepsilon f(y,z)]$$

where $\varepsilon \equiv \frac{\Delta}{L_x}$, $f(y,z) \equiv -\frac{4}{L_y}(y-\frac{3}{4}L_y) [U (y-\frac{3L_y}{4}) - U(y-L_y)]$.

Differentiating p_{020} and $f(y,z)$ with respect to y, gives

$$\frac{\partial p_{020}}{\partial y} = -\frac{2\pi P}{L_y} \sin \frac{2\pi}{L_y} y \cos (2wt+\theta_2),$$

and

$$\frac{\partial f(y,z)}{\partial y} = -\frac{4}{L_y} [U(y - \frac{3L_y}{4}) - U(y-L_y)]$$

$$- \frac{4}{L_y} (y - \frac{3}{4} L_y) [\delta(y - \frac{3L_y}{4})$$

$$- \delta(y-L_y)] \qquad (3)$$

Equation (3) is substituted into the following Equation (4),

$$\frac{\partial P'}{\partial x} \Big|_{x=L_x} = L_x [\frac{\partial f(y,z)}{\partial y} \frac{\partial p_{020}}{\partial y}]_{x=L_x}$$

giving

$$\frac{\partial p'}{\partial x} \Big|_{x=L_y} = A \sin \frac{2\pi}{L_y} y \cos (2wt + \theta_2) [U(y-\frac{3L_y}{4}) - U(y-L_y)$$

$$+ (y-\frac{3}{4}L_y) [\delta(y-\frac{3L_y}{4}) - \delta(y-L_y)]] \qquad (4)$$

where $A \equiv \frac{8\pi P L_x}{L_y^2}$.

Equation (4) can be expanded as a Fourier series.

$$\frac{\partial P'}{\partial x} \Big|_{x=L_x} = A \cos (2wt + \theta_2) [\sum_{m=0}^{\infty} A_m \cos \frac{m\pi}{L_y} y$$

$$+ \sum_{m=1}^{\infty} b_m \sin \frac{m\pi}{L_y} y] \qquad (5)$$

Only A_o needed to determine the first order correction term due to the degerate between (0,2,0) and (1,0,0) modes.

$$A_o = \frac{1}{L_y} \int_o^{L_y} \sin \frac{2\pi}{L_y} y \left\{ U\left(y-\frac{3L_x}{4}\right) - U(y-L_y) \right.$$

$$\left. + \left(y - \frac{3}{4} L_y\right) \left[\delta\left(y-\frac{3}{4}L_y\right) - \delta(y-L_y)\right] \right\} dy$$

$$= \frac{1}{2\pi}$$

So the perturbation correction, P' is

$$p' = \frac{2A\, A_o}{L_x \left(\frac{2w}{C_o}\right)^2} Q_{100} \sin \tau_{100} \cos \frac{\pi x}{L_x} e^{i(2wt + \theta_2 + \tau_{100})} \quad (6)$$

The pressure at microphone position, $x=L_x$, can be written as following with $\left(\frac{2w}{C_o}\right)^2 = \left(\frac{4\pi}{L_y}\right)^2$,

$$P_{mic} = P_{020} + \varepsilon p' = P\mathrm{Re}\left[e^{i(2wt + \theta 2)} + \frac{1}{\pi} \varepsilon A_o P_{100} \sin \tau_{100} x \right.$$

$$\left. e^{i(2wt + \ 2 + \tau_{100})} \right] \quad (7)$$

The total pressure amplitude at a microphone position will be

$$|P_{mic}| = P\sqrt{(1+B\cos \tau_{100})^2 + (B \sin \tau_{100})^2} \quad (8)$$

where $B = \frac{1}{\pi} \varepsilon A_o Q_{100} \sin \tau_{100}$

[In reference [4], the author made a error in formulating Equation (2); he used y instead of $(y-aL_x)$ and got an incorrect value of A_o.]

V. APPARATUS

A. THE RECTANGULAR CAVITY

The cavity is constructed from 0.75 inch aluminum (Fig. 1). The interior of dimension of the cavity is 12.002 inches long, 2.5002 inches high with a width that can be varied between 5.50 inches to 7 inches in 0.25 inch increments. It was sealed by a thin silicon grease layer prior to assembly. There are three different microphone positions for the purpose of discriminating the different modes.

Figure 2 shows the pressure distribution for several of the lower modes. According to Table I (calculated for cavity dimensions, 12"x6"x2.5"), the (0,2,0) and (1,0,0) modes are degenerate. Experimentally (0,2,0) mode was about 3 Hz higher than (1,0,0) mode.

The piston is set flush with the bottom of the cavity as near to the wall Y=0 as practically possible, and halfway between the wall at X=0 and X=L_x. In this position it can excite the (0,n,0) family of modes but it cannot excite the (1,0,0) mode. To drive the (1,0,0) mode it is necessary to insert an auxilliary driver (ID-30) at Position A. A microphone at Position B will sense the pressure of all modes. It determines the resonance

frequencies and Q's of the degenerate modes. The microphone is placed at Position A to sense the (1,0,0) mode without contamination from the (0,2,0) and at Position C to sense the (0,2,0) mode without contamination from the (1,0,0) mode.

B. BLOCK DIAGRAM (Fig. 4)

GR 1161-A coherent decade frequency synthesizer produces a driving signal which is precise to $\pm$0.001 Hz. This signal enters a 2120 MB power amplifier which drives the shaker. The piston motion was continuously monitored by an Endevco Model 2215 Accelerometer mounted within the piston, measured on a HP 400D Voltmeter and the output of the accelerometer was observed qualitatively on a Model 13D BR HP oscilloscope. A Schlumberger spectrum analyzer was used to check for harmonic distortion in the piston motion.

The output of a microphone with matching preamplifier B&K 2801 fed into the three devices; (1) HP 400D VTVM for measuring overall voltage leve, (2) the spectrum analyzer for analyzing the wave component, and (3) two HP 302A wave analyzers for measuring the pressure of the first two harmonics.

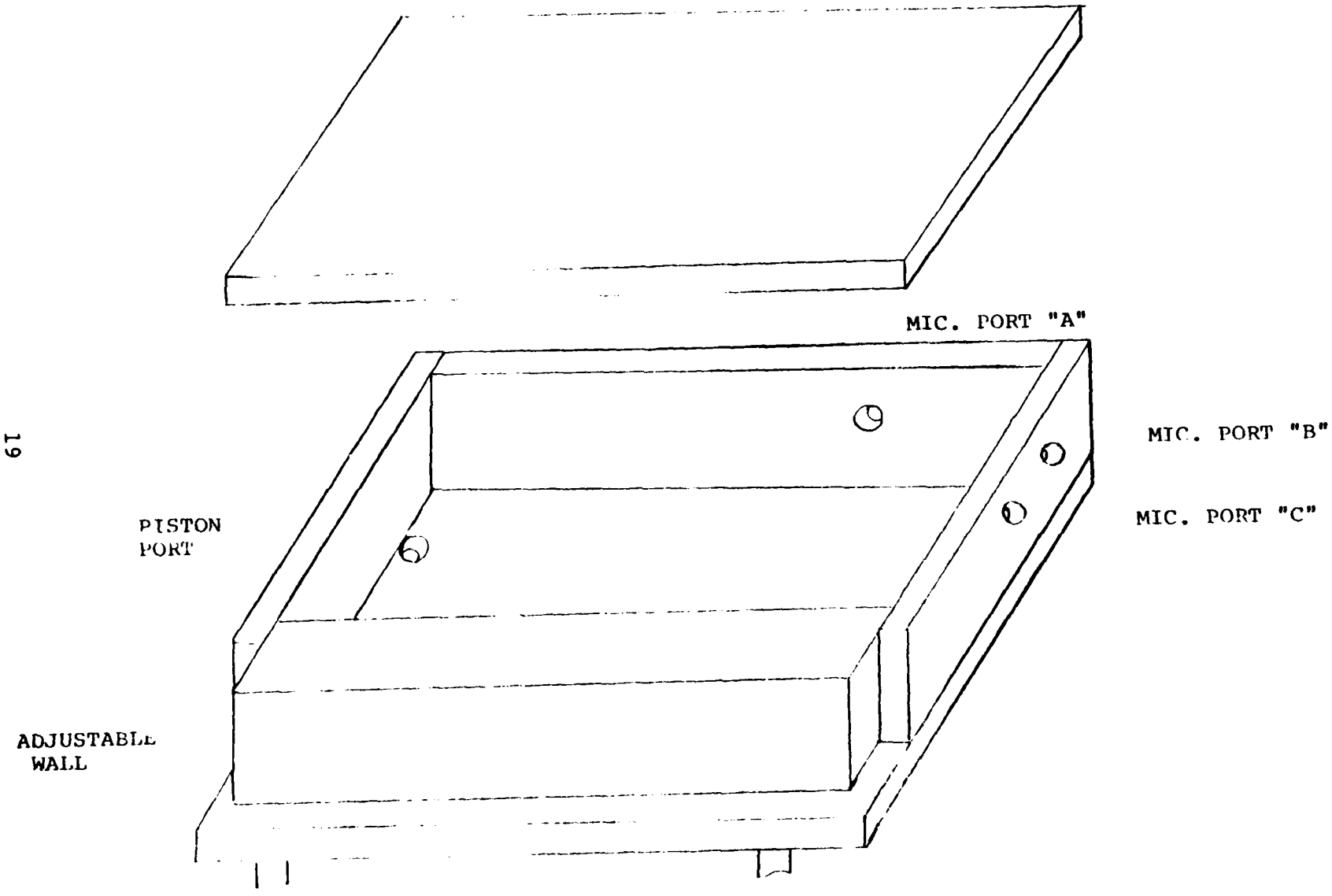

Fig. 1. Adjustable Rectangular Cavity

TABLE I

Mode	Frequency (Hz)	Mode	Frequency (Hz)
010	565	130	2039.4
020	1131	140	2529.0
030	1697	150	3032.0
100	1131	111	2980.5
110	1205	101	2757.5
120	1599.5	011	2926.4

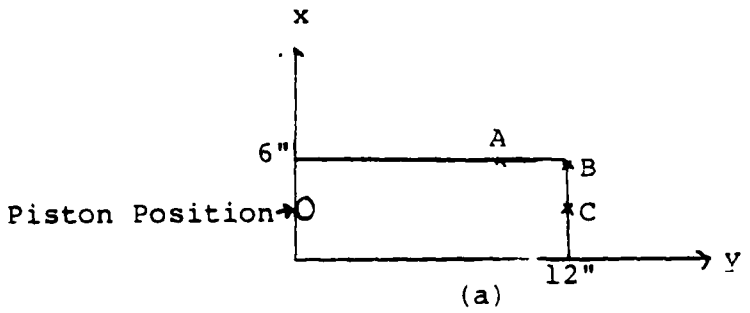

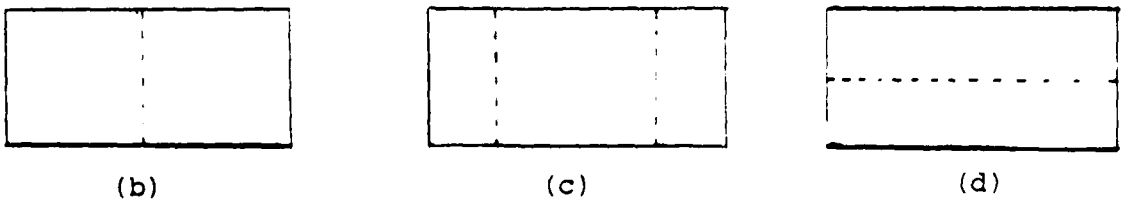

Fig. 2. (a) Cavity Orientation, (b) Pressure Nodes for (0,1,0), (c) For (0,2,0), (d) For (1,0,0).

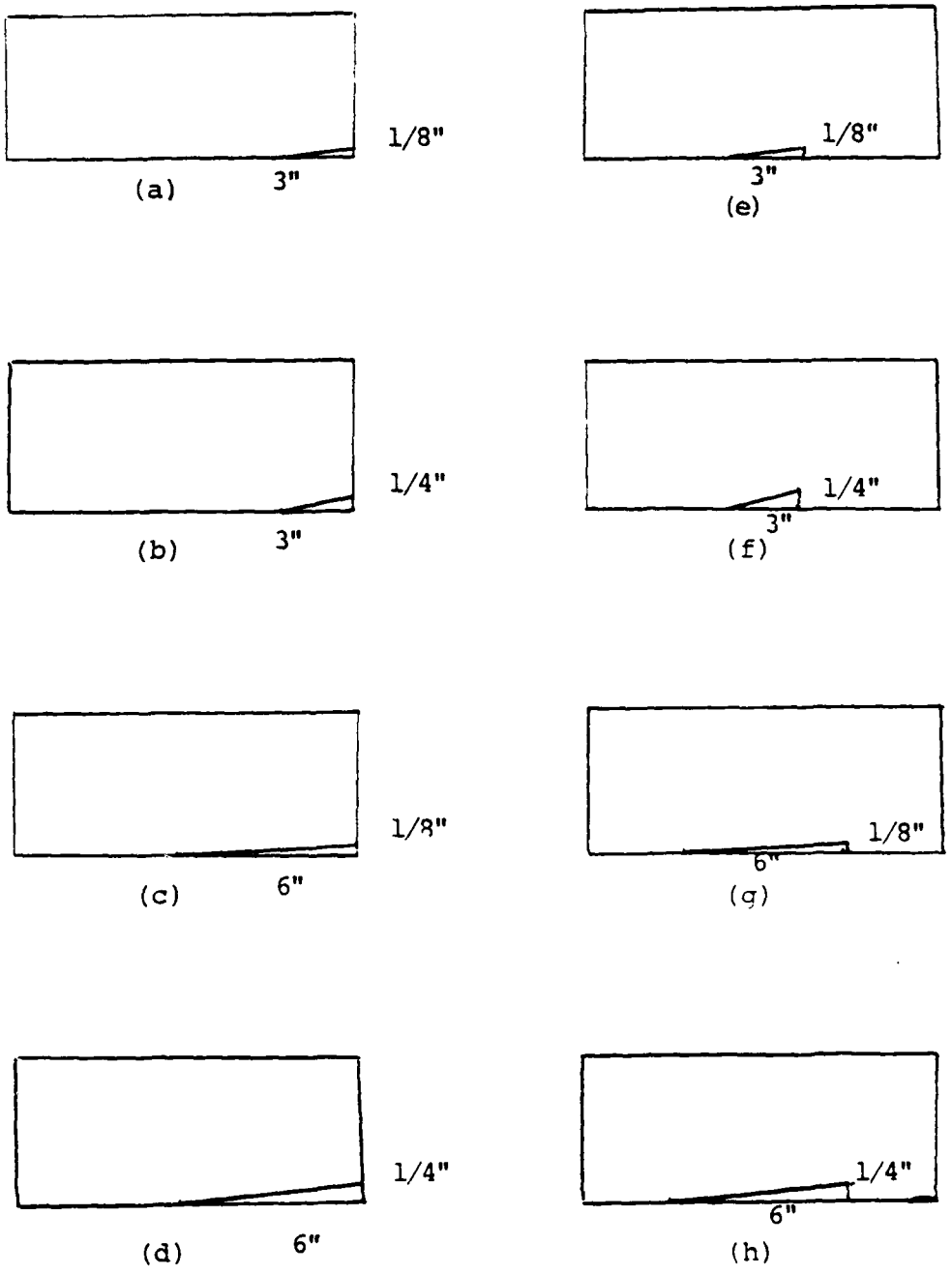

Fig. 3. Perturbation Configuration

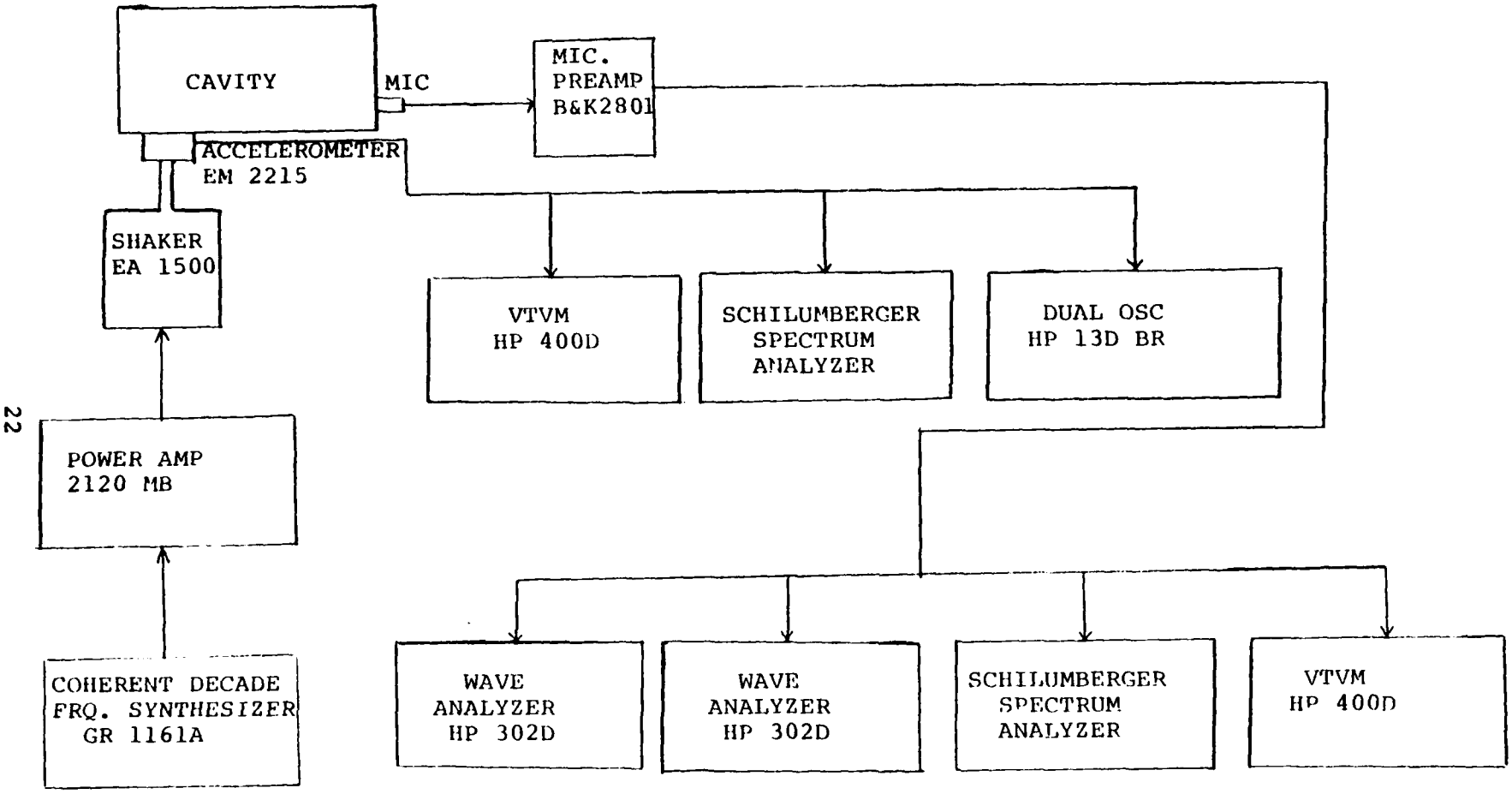

Fig. 4. Block Diagram

VI. DATA COLLECTION PROCEDURE

Since the resonance frequencies of the cavity was observed to drift with time, the system was allowed warm-up for at least one hour prior to data collection. The harmonic content of the accelerometer output was analyzed and the piston was adjusted until the second harmonic of the accelerometer output was at least 50 dB below that of the fundamental frequency. Figure 5 shows typical results for piston V_2/V_1 in the region of the finite amplitude measurement. For a driving voltage typical of those used in the experiment, measurements were limited to those frequencies for which $V_2/V_1 < 1\%$.

There are three measurement procedures for collecting data; (1) a pre-run infinitesimal amplitude measurement, (2) the finite amplitude measurement, and (3) a post-run infinitesimal measurement.

A. PRE-RUN AND POST-RUN INFINITESIMAL MEASUREMENTS

During these measurements, the piston was driven so that accelerometer output was less than 0.1 v. The resonant frequency of the fundamental and the Q factor first few (0,n,0) in the modes were determined from

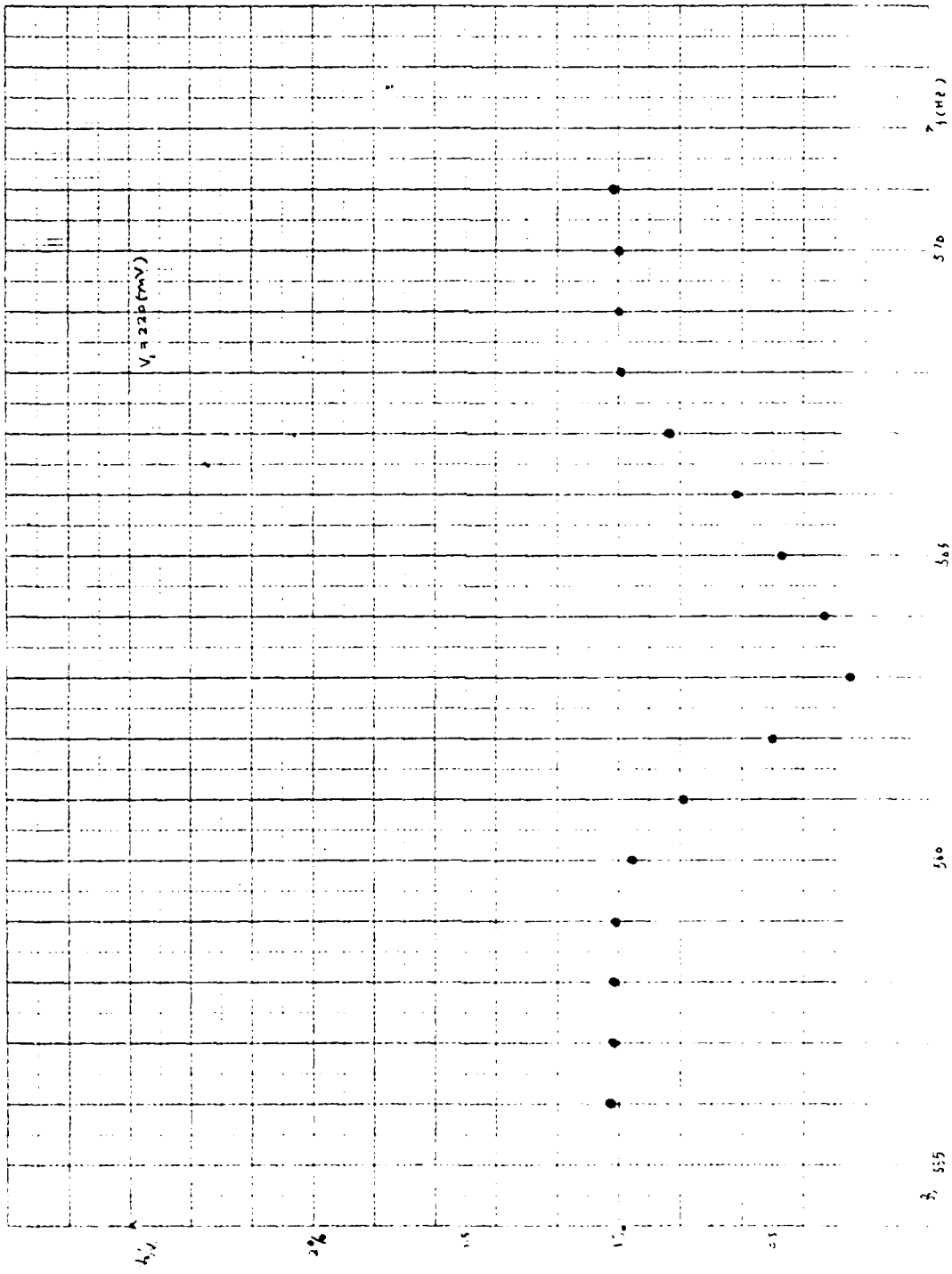

Figure 5

$$f_r = \frac{f_u - f_L}{2}$$

$$Q = \frac{f_r}{f_u - f_L}$$

The resonance frequency and Q of (1,0,0) were determined by driving the cavity at port "A:.

The harmonicity coefficients were then calculated from

$$E_n = \frac{f_n - nf_1}{nf_1} \text{ , for } E_{ono}$$

$$= \frac{f_r - f_2}{f_2} \text{ , for } E_{100}$$

The times at which f_u and f_L were taken was recorded.

B. THE FINITE AMPLITUDE MEASUREMENT

Throughout this measurement V_1 had to be kept constant which required adjustment of the driving voltage applied to the piston. The HP 302A wave analyzer was set to the driving frequency and the driving voltage adjusted to keep V_1 constant as the frequency was changed with the microphone in Postion B. The frequency was increased 0.5 Hz steps through ± 6 Hz about the resonance frequency of a fundamental mode. At each driving frequency, the harmonic content of the microphone onput, usually up to the fourth, was measured with HP 302A wave analyzer set on AFC mode and the time of that measurement recording

presented. The results were presented as V_n/V_1 vs. the frequency parameter for a given strength parameter and perturbation.

To determine the exact value of the frequency parameter, the value of f_r at the instant of the measurement of V_n was determined by interpolation of the values of f_n found in the pre- and post-run procedures. Figure 6 shows the drift in f_r is approximately linear in time.

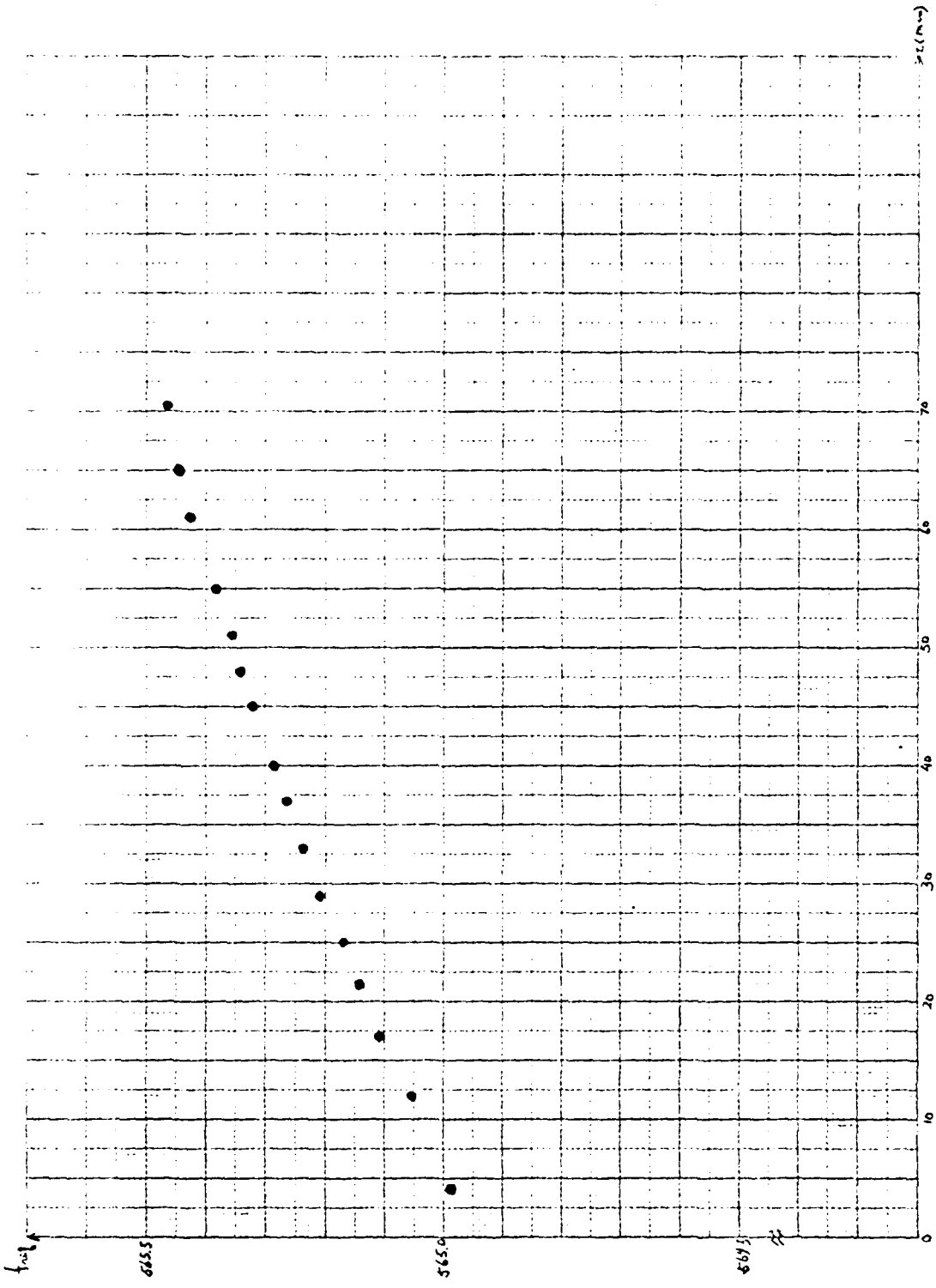

Figure 6

VII. RESULTS

Figure 7 shows the excellent agreement between theory and experiment obtained when there are no perturbations so that only one family of modes is excited.

Some discrepancies were always observed when the driving frequency was far from the fundamental resonance frequency (for $|FP|<2.$) In this region, the piston had to be driven hard to keep V_1 constant. This causes a second harmonic to appear in the piston waveform (as shown by Fig. 3), thereby introducing a linearly-generated second harmonic into the cavity.

For the boundary perturbation of Fig. 3, the results are plotted in Figs. 8 through 15. The thin line is the theory prediction for the perturbation and the thick line includes the perturbation correction. The small circles are experimental results. Along the edge of each figure is the information about the cavity configuration.

A. THE WEDGE AT THE CORNER OF THE CAVITY

Figures 8 through 11 show the results for a wedge at the corner of the cavity. The wedge used are those of Fig. 3 (a)-(d) respectively.

B. THE WEDGE AT THE CENTER OF THE LONG WALL

Figures 12 through 15 show the results for the same wedges (Fig. 3 (a)-(h)) but now located at the center of

the long wall. For Figures 12 and 13, A_o = 0.177 with DELTA for Figure 13 twice that for Figure 12. For Figures 14 and 15, A_o = 0.500 with DELTA the same as for Figures 12 and 13.

VIII. CONCLUSIONS

A. The experimental apparatus and procedures are capable of providing data sufficiently precise to verify the prediction of the theory in the absence of geometrical perturbation if the range of driving frequencies is restricted so that the absolute value of the frequency parameter is less than 2.

B. To verify the correction for a geometrical perturbation, it is useful to have: (1) a sufficiently large correction to the unperturbed prediction and (2) the sign of the correct must change for an absolute value of the frequency parameter less than 2.

C. The experimental results show that geometrical perturbation alters the finite amplitude behavior of the cavity, and that the nature these change are in qualitative agreement with the predictions of the theory. However, quantitative agreement was not observed.

D. Sources of the difficulties in obtaining good agreement might be; (1) the inability to experimentally satisfy conditions of B above, (2) the DELTA function arising from the perturbations used may cause trouble in the theory (Also, they may be difficult to accurately reproduce experimentally.), and (3) the higher order terms neglected in developing the theory may not all be

small. For example, terms of order higher than first order in Equation (4) of Section II and terms of order higher than A_o and all b_m in Equation (5) of Section IV.

E. The theory for the perturbed cavity can probably be critically tested, if a perturbation shape is used that avoids the difficulties of D(2) and satisfies the condition of B. At this time it is not obvious that such a perturbation can be found, but there seems to be no fundamental obstacle to find a suitable perturbation.

APPENDIX A

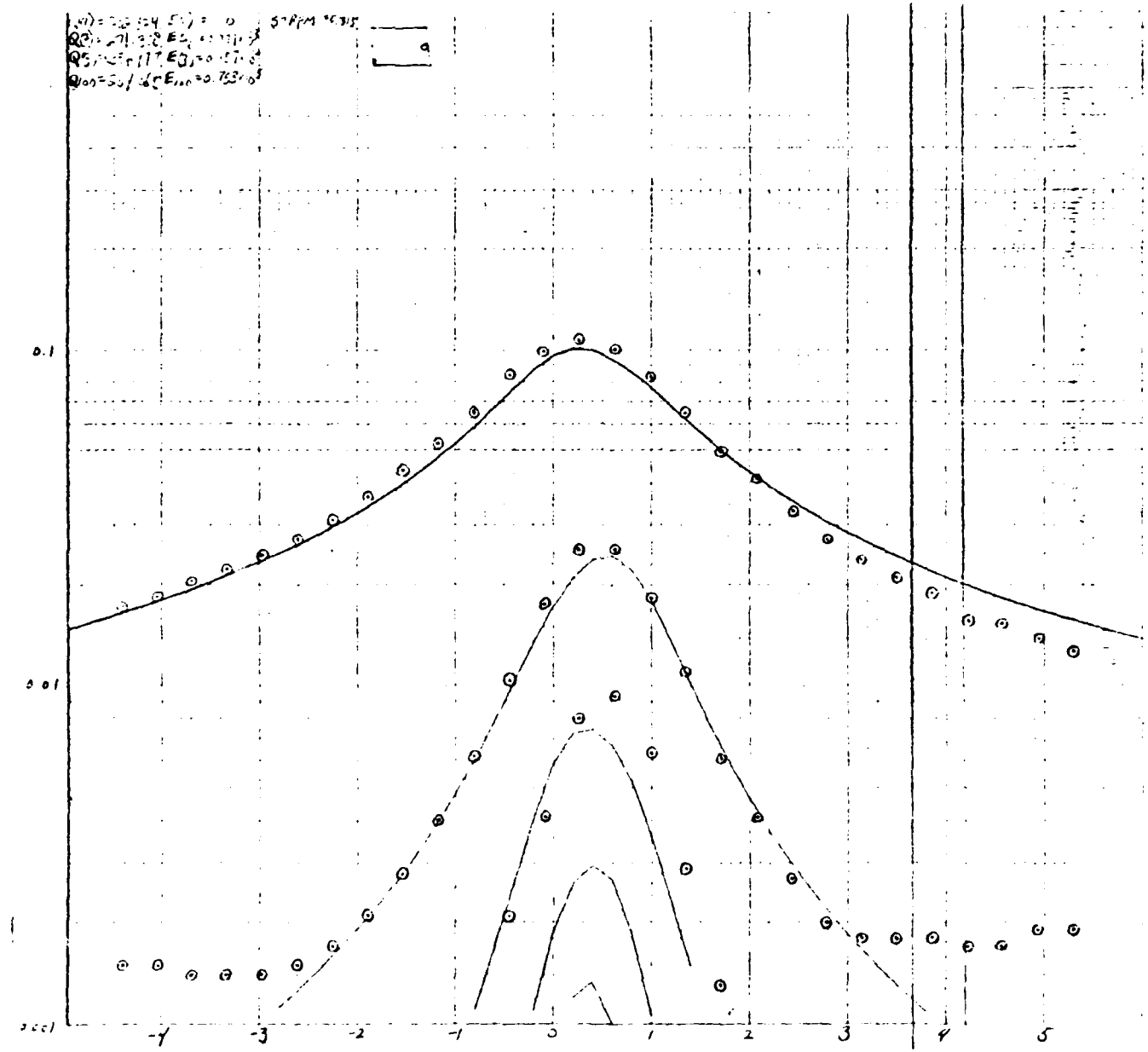

Fig. 7

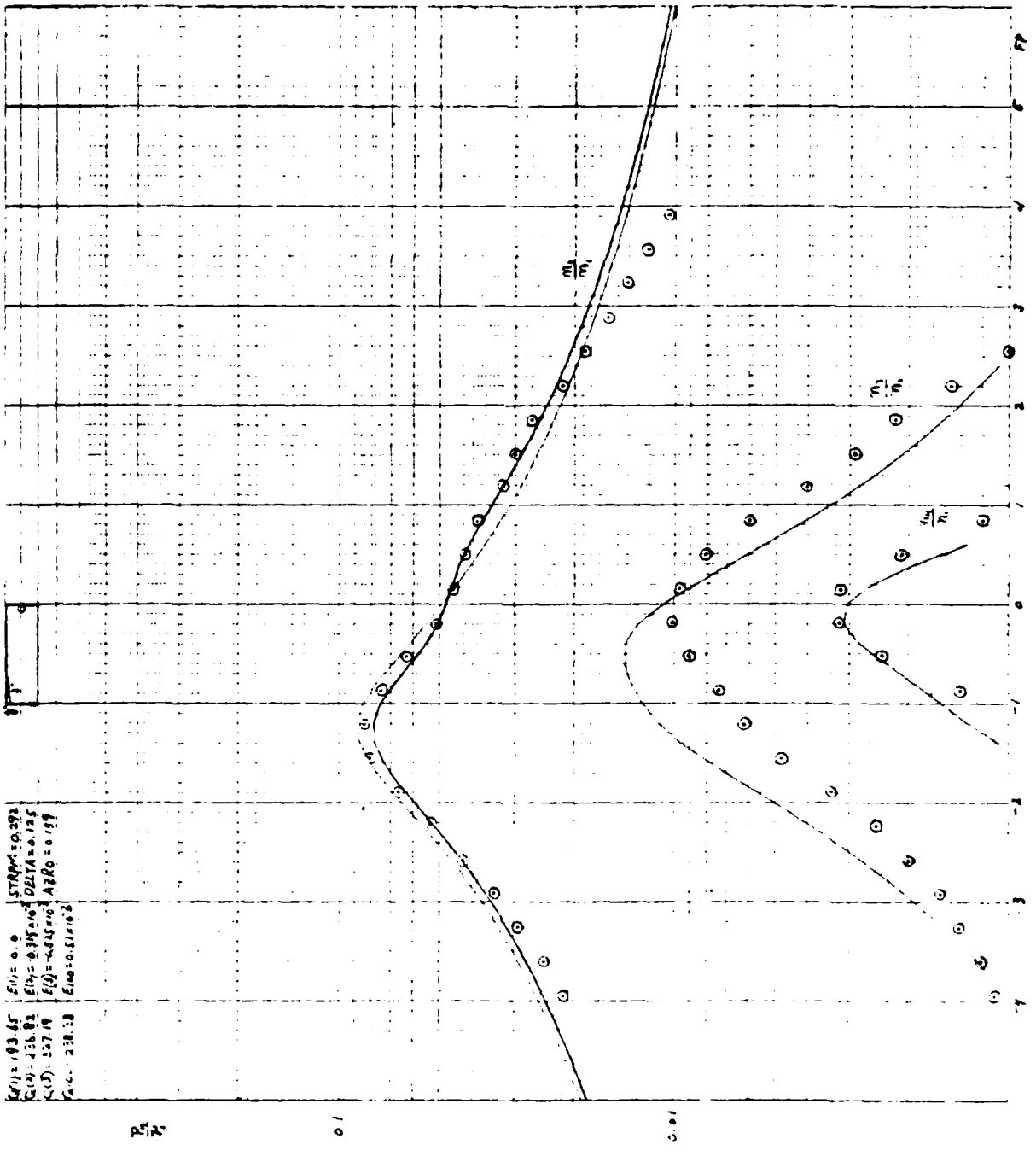

Fig. 8

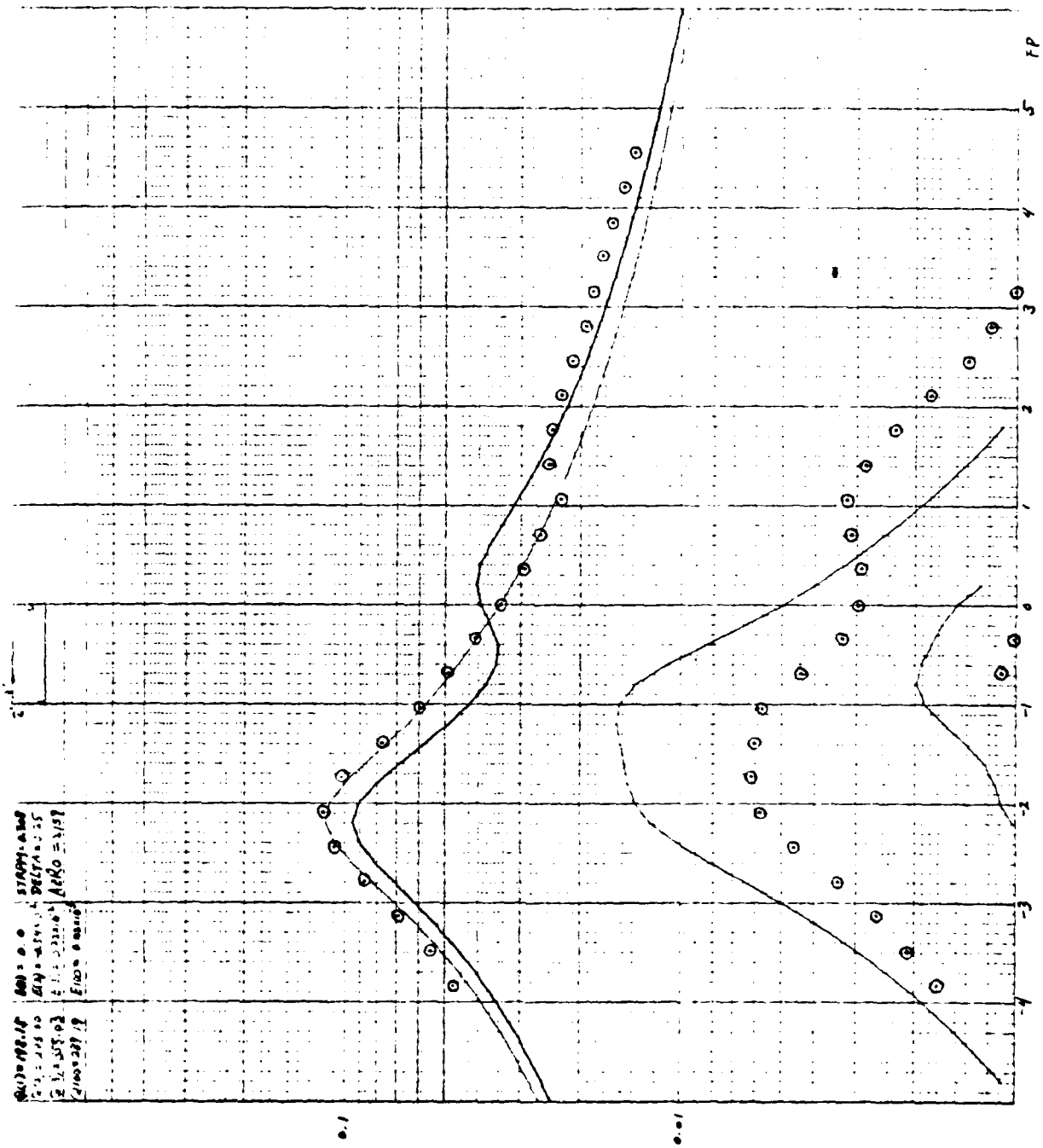

Fig. 9

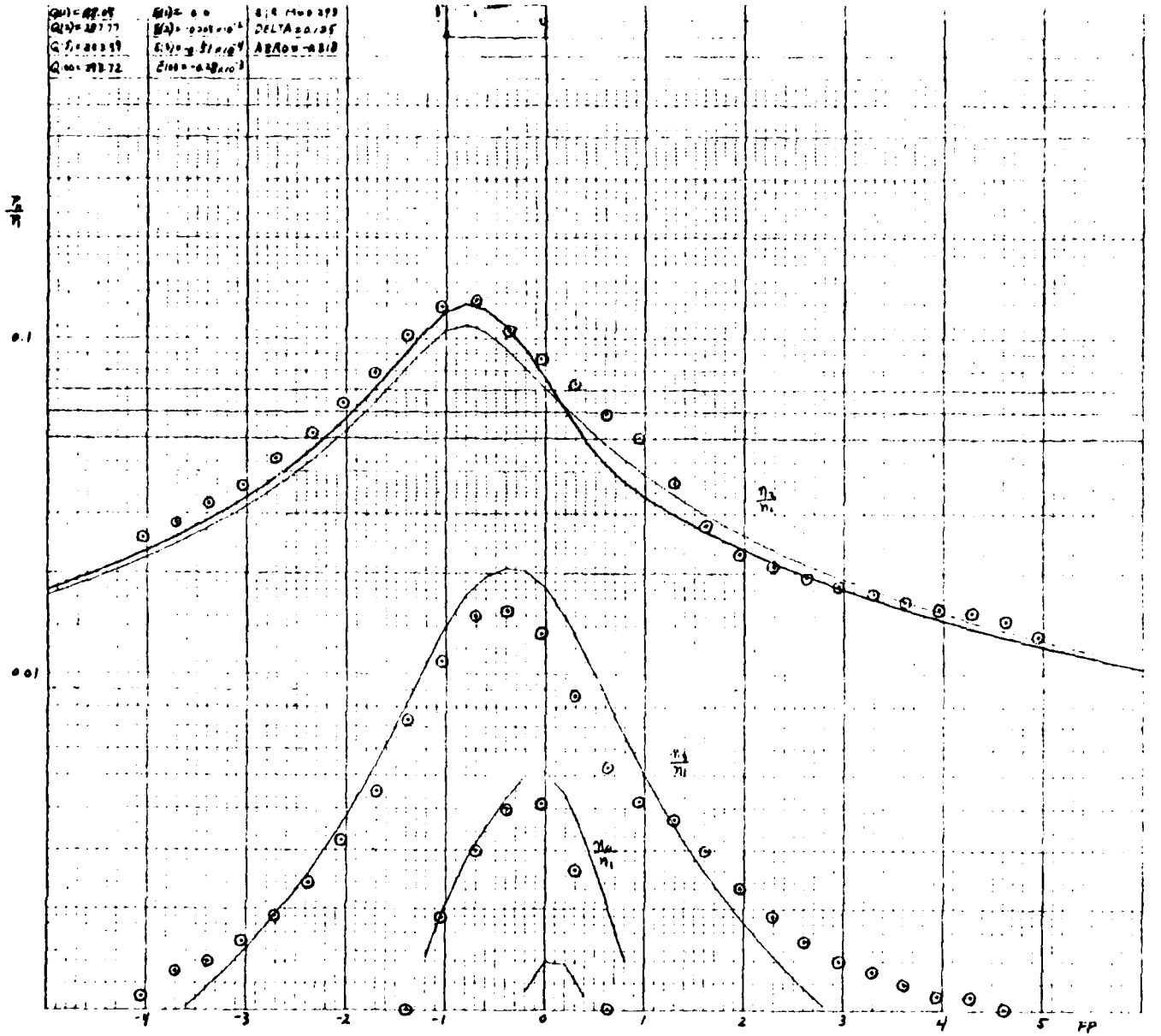

Fig. 10

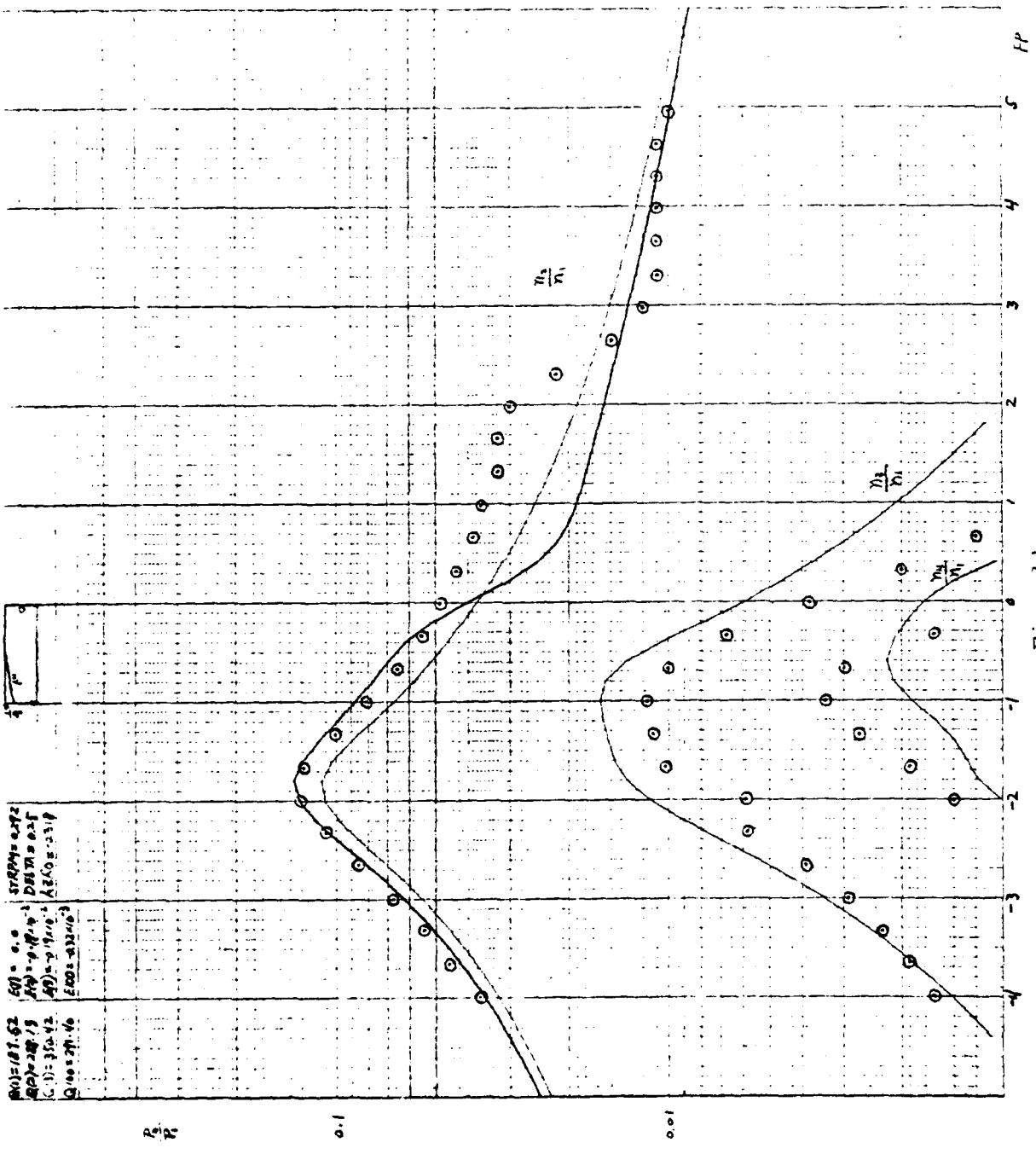

Fig. 11

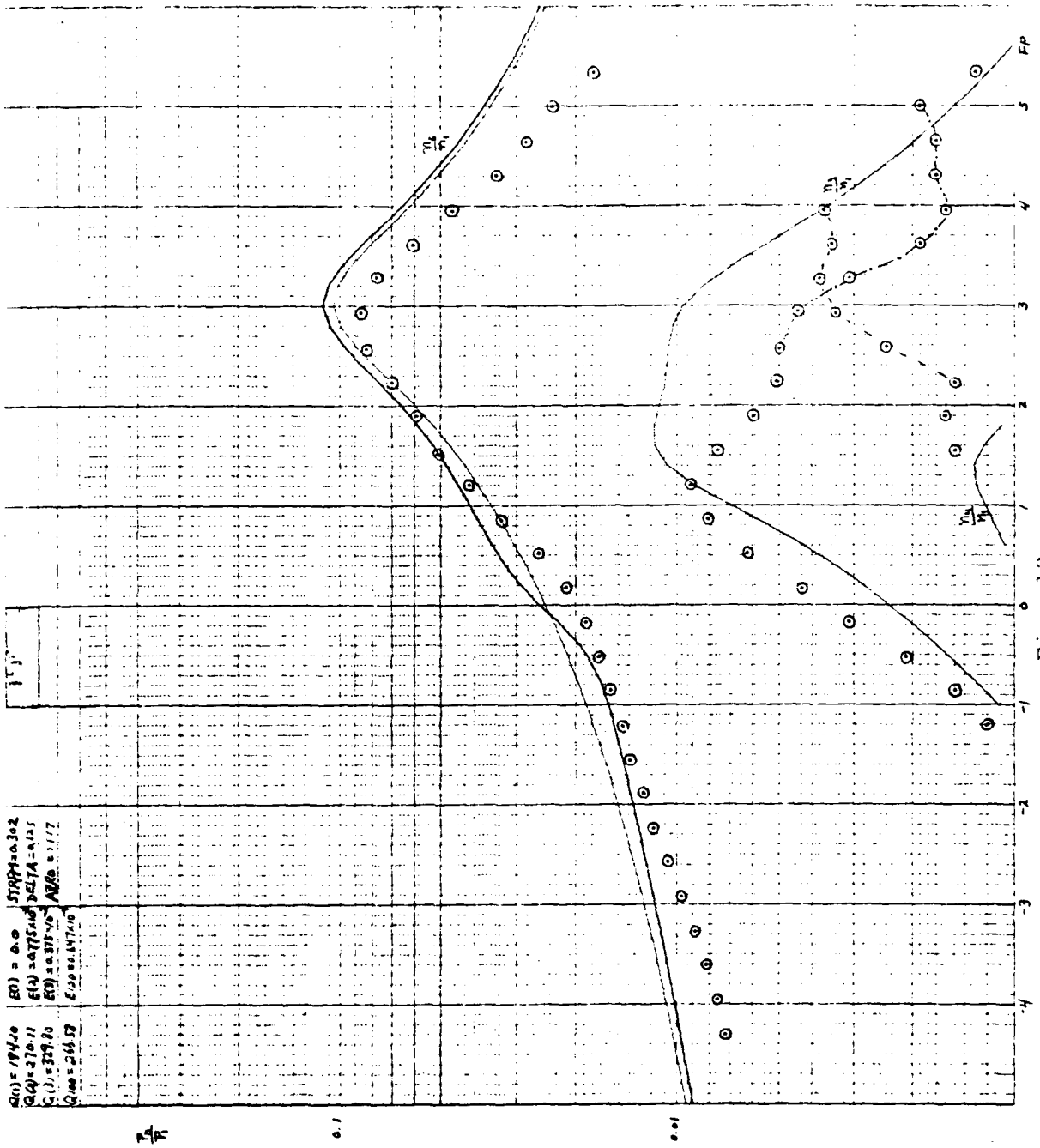

Fig. 12

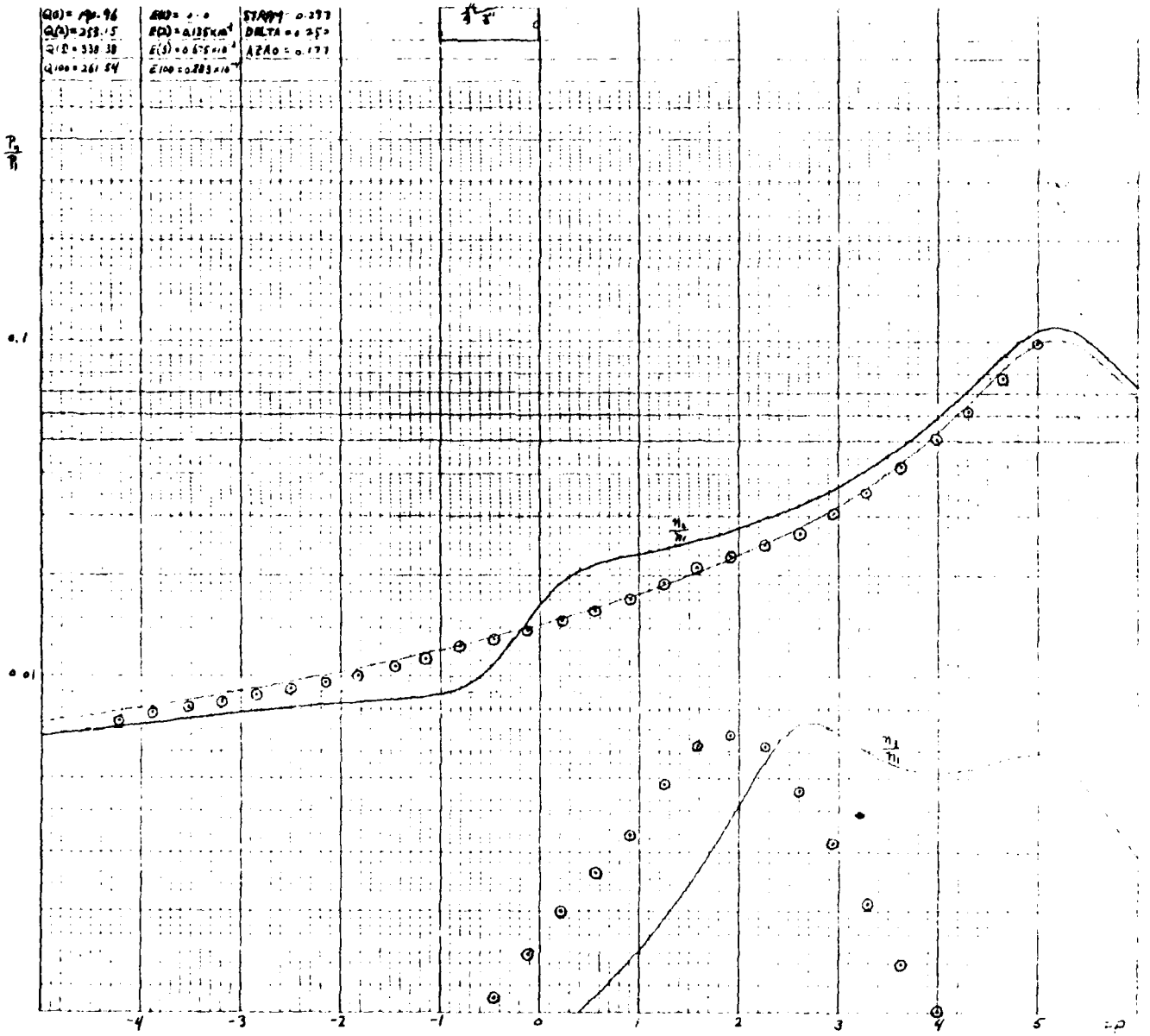
Q(0) = 496.96
Q(1) = 253.15
Q(2) = 338.38
Q(100) = 261.84
STARPH 0.277
DELTA = 0.25°
AZAO = 0.171
0.1
0.01
-4
-3
-2
-1
0
1
2
3
4
5

Fig. 13

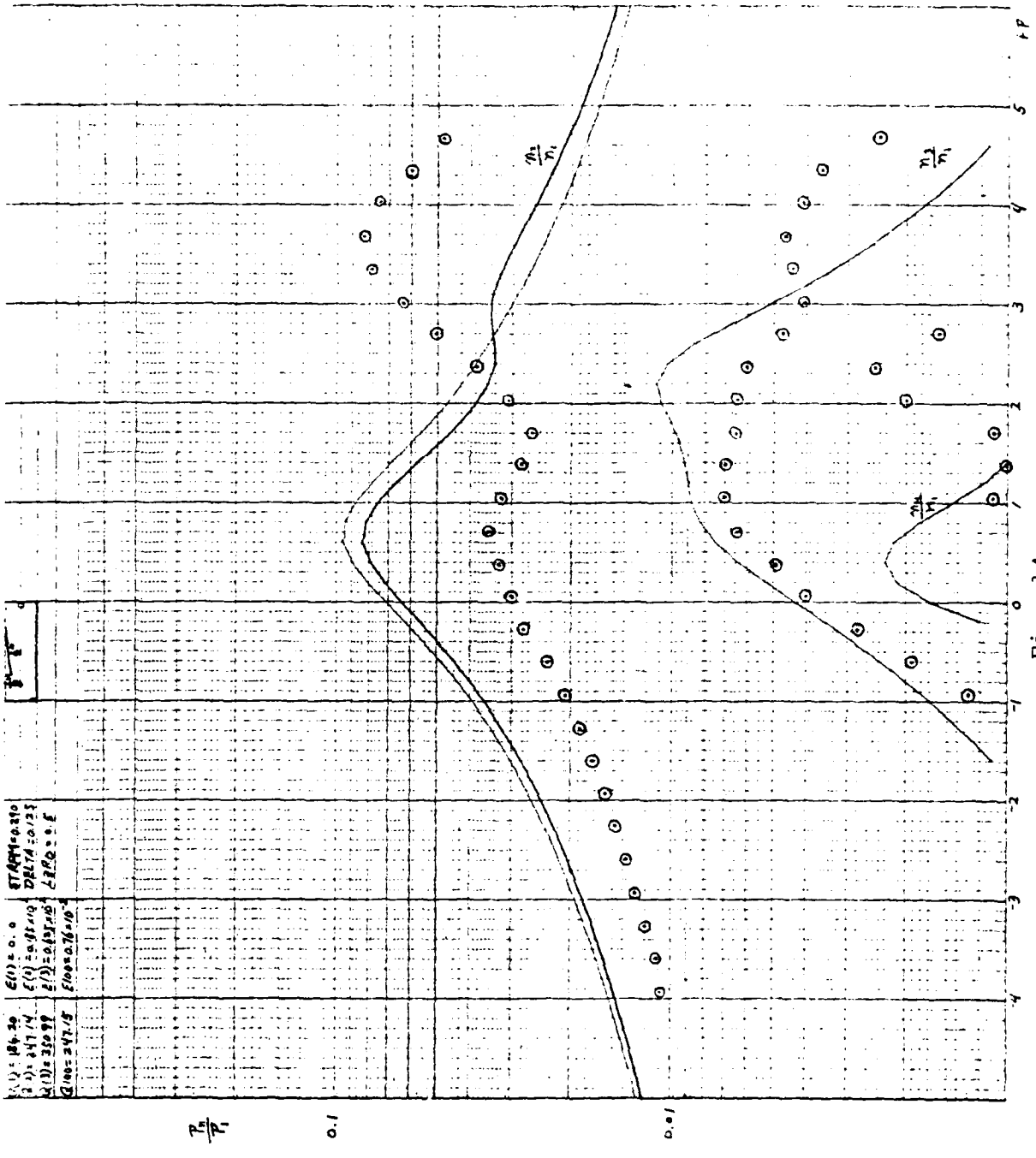

Fig. 14

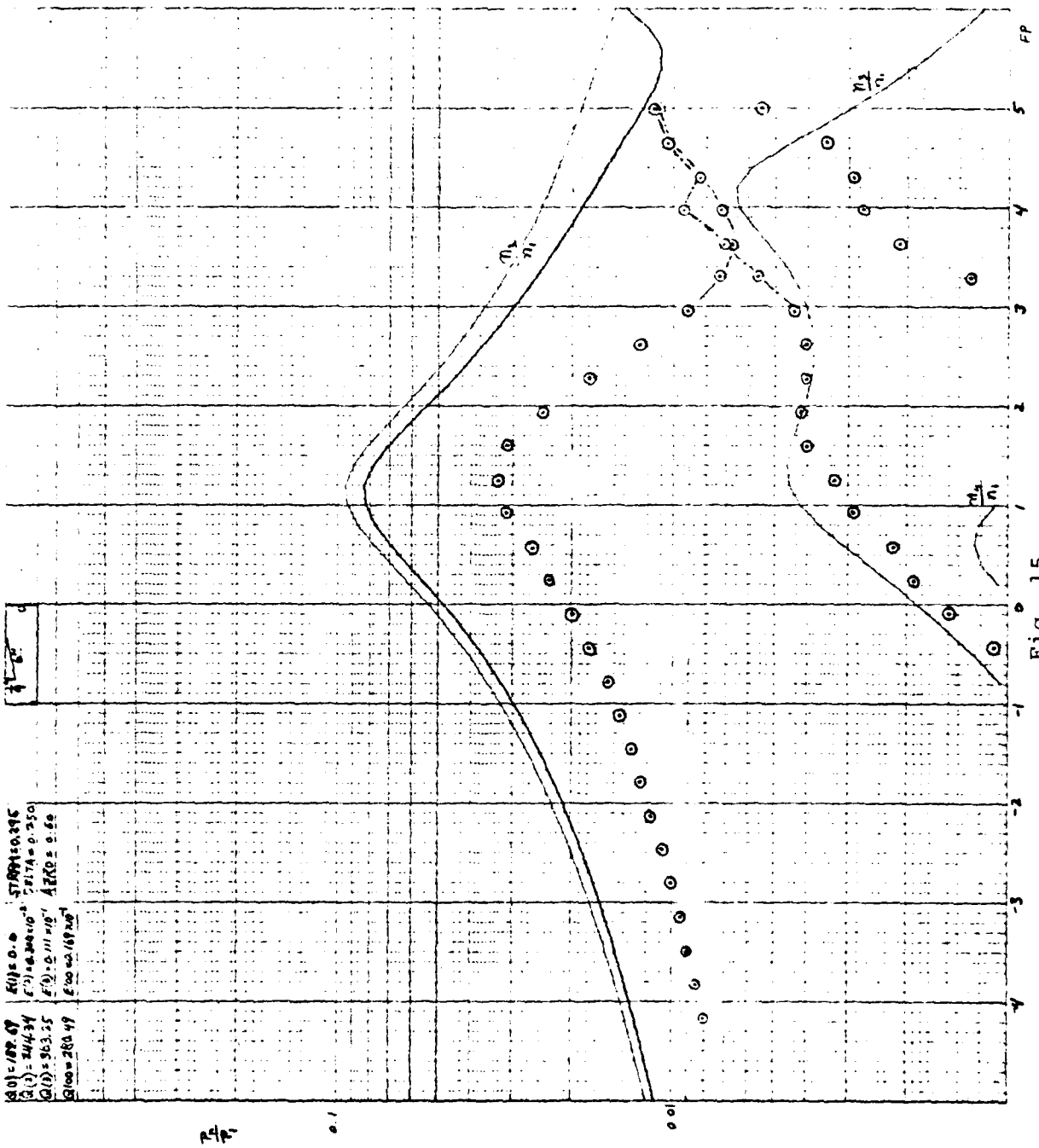

Fig. 15

APPENDIX B

TABLE I (Fig. 7)

mode	time	f_u	f_L	f_r	Q	E
010	0	565.77	562.88	564.33	195.40	0
020	3	1131.84	1127.79	1129.81	278.69	0.10×10^{-2}
030	6	1698.27	1693.52	1695.90	356.51	0.17×10^{-2}
100	9	1131.87	1127.59	1129.73	264.20	-0.74×10^{-4}

V_1 = 11dB time	f	V_2	V_3	V_4	P_2/P_1	P_3/P_1	$P_4/P_.$	FP
12	558.5	-50.0	-70.5	-70.5	0.0113	0.0011	0.0011	-4.19
13	559.0	-47.9	-72.0	-69.0	0.0143	0.0009	0.0013	-3.85
14	559.5	-46.9	-73.8	-67.8	0.0160	------	0.0014	-3.50
15	560.0	-46.0	-72.6	-67.5	0.0179	------	0.0015	-3.15
16	560.5	-44.8	-71.2	-69.7	0.0204	0.0011	0.0012	-2.81
17	561.0	-43.7	-69.7	-73.5	0.0233	0.0012	------	-2.47
18	561.5	-42.4	-67.8	-76.5	0.0269	0.0014	------	-2.12
19	562.0	-41.0	-65.7	-75.9	0.0316	0.0018	------	-1.78
20	562.5	-39.4	-63.2	-82.5	0.0380	0.0025	------	-1.43
21	565.0	-37.8	-60.3	-85.0	0.0457	0.0034	------	-1.09
22	563.5	-35.9	-56.6	-74.9	0.0569	0.0052	------	-0.74
23	564.0	-34.0	-52.2	-67.5	0.0708	0.0007	0.0015	-0.40
24	564.5	-32.2	-47.6	-60.6	0.0876	0.0148	0.0033	-0.05
25	565.0	-31.1	-45.0	-54.5	0.0994	0.0200	0.0067	0.29
26	565.5	-31.6	-43.9	-52.9	0.0933	0.0226	0.0081	0.64
27	566.0	-33.3	-46.7	-56.0	0.0772	0.0164	0.0056	0.98
28	566.5	-35.3	-51.0	-63.2	0.0610	-0.0100	0.0025	1.33
29	567.0	-37.6	-55.5	-70.8	0.0484	0.0060	0.0010	1.67
30	567.5	-39.8	-60.0	-73.6	0.0365	0.0036	------	2.02
31	568.0	-42.1	-64.3	-74.7	0.0279	0.0022	------	2.36
32	568.5	-44.1	-68.5	-74.2	0.0221	0.0013	------	2.71
33	569.0	-46.2	-69.9	------	0.0174	0.0011	------	3.05
34	569.5	-47.2	-68.7	-67.0	0.0156	0.0013	0.0016	3.40
35	570.0	-48.0	-65.4	-67.0	0.0141	0.0019	0.0010	3.14
36	570.5	-48.9	-65.1	-67.2	0.0127	0.0020	0.0016	4.09
37	571.0	-49.8	-65.2	-67.5	0.0115	0.0019	0.0015	4.43
38	571.5	-50.8	-65.4	-68.2	0.0103	0.0019	0.0014	4.78
39	572.0	-51.7	-65.8	-68.6	0.0093	0.0018	0.0013	5.12
40	572.5	-52.5	-66.3	-67.4	0.0084	0.0017	0.0015	3.47
41	573.0	-54.7	-65.1	-66.7	0.0065	0.0020	0.0016	5.81

mode	time	f_u	f_L	f_r	Q	E
010	44	566.28	563.37	564.82	194.03	0
020	47	1132.74	1128.67	1130.71	277.82	0.94×10^{-3}
030	50	1699.77	1694.97	1697.37	353.84	0.17×10^{-2}
100	53	1132.80	1128.48	1130.64	262.03	-0.61×10^{-4}

TABLE II (Fig. 8)

mode	time	f_u	f_L	f_r	Q	E
010	0	568.27	565.28	566.77	189.81	0
020	3	1132.37	1127.62	1129.99	238.25	-0.31×10^{-2}
030	6	1701.89	1696.79	1699.34	333.14	-0.57×10^{-3}
100	9	1132.44	1127.71	1130.07	238.76	0.69×10^{-4}

V_1=-11dB	time	f	V_2	V_3	V_4	P_2/P_1	P_3/P_1	P_4/P_1	FP
	12	561.3	-44.3	-69.9	-71.3	0.0216	0.0011	———	-3.95
	13	561.8	-43.2	-69.2	-72.2	0.0247	0.0012	———	-3.61
	14	562.3	-41.7	-68.3	-74.0	0.0293	0.0014	———	-3.26
	15	562.8	-40.2	-66.8	-80.0	0.0347	0.0016	———	-2.92
	16	563.3	-38.5	-65.2	———	0.0422	0.0020	———	-2.58
	17	563.8	-36.4	-62.9	———	0.0537	0.0025	———	-2.24
	18	564.3	-34.3	-60.3	———	0.0684	0.0034	———	-1.90
	19	564.8	-32.8	-57.2	———	0.0813	0.0049	———	-1.56
	20	565.3	-32.5	-55.0	-72.0	0.0841	0.0063	0.0009	-1.22
	21	565.8	-33.5	-53.5	-67.8	0.0750	0.0075	0.0014	-0.87
	22	566.3	-35.1	-51.8	-62.5	0.0624	0.0092	0.0024	-0.53
	23	566.8	-36.9	-50.9	-60.9	0.0507	0.1002	0.0032	-0.19
	24	567.3	-37.9	-51.2	-60.8	0.0452	0.0098	0.0032	0.15
	25	567.8	-38.6	-52.8	-64.6	0.0419	0.0082	0.0021	0.49
	26	568.3	-39.2	-55.3	-69.2	0.0391	0.0061	0.0072	0.83
	27	568.8	-40.3	-58.7	-75.0	0.0343	0.0041	———	1.78
	28	569.3	-41.5	-61.7	-78.5	0.0300	0.0029	———	1.52
	29	569.8	-42.4	-64.3	———	0.0271	0.0022	———	1.86
	30	570.3	-44.3	-67.3	———	0.0218	0.0015	———	2.20
	31	570.8	-45.5	-70.8	———	0.0188	0.0010	———	2.54
	32	571.3	-46.9	-75.0	———	0.0160	0.0006	———	2.88
	33	571.8	-48.1	-76.9	———	0.0140	0.0005	———	3.22
	34	572.3	-49.3	-75.2	-69.1	0.0122	0.0006	0.0012	3.57
	35	572.8	-50.6	-73.5	-68.0	0.0105	0.0007	0.0014	3.91
	36	573.3	-51.0	-71.7	-66.5	0.0100	0.0009	0.0017	4.2[illegible]
	37	573.8	-51.8	-71.1	-66.0	0.0092	0.0010	0.0018	4.5[illegible]
	38	574.3	-52.5	-70.3	-65.7	0.0084	0.0011	0.0019	4.93
	39	574.8	053.8	-72.3	-66.7	0.0073	0.009	0.0016	5.27

mode	time	f_u	f_2	f_r	Q	E
010	42	568.82	565.95	567.38	197.49	0
020	45	1133.50	1128.70	1131.10	235.40	-0.32×10^{-2}
030	48	1703.98	1698.69	1701.34	321.25	-0.48×10^{-3}
100	51	1133.85	1129.10	1131.47	238.00	0.33×10^{-3}

TABLE III (Fig. 9)

mode	time	f_u	f_2	f_r	Q	E
010	0	567.85	565.01	566.43	199.52	0
020	3	1128.61	1124.81	1126.71	296.58	-0.54×10^{-2}
030	6	1697.95	1693.16	1695.39	354.31	-0.23×10^{-2}
100	9	1128.77	1124.87	1126.82	288.63	-0.96×10^{-4}

V_1=-11dB time	f	V_2	V_3	V_4	P_2/P_1	P_3/P_1	P_4/P_1	FP
12	561.0	-37.6	-66.2	———	0.0468	0.0017	———	-3.84
13	561.5	-36.2	-64.8	———	0.0550	0.0021	———	-3.49
14	562.0	-34.3	-62.8	———	0.0684	0.0026	———	-3.14
15	562.5	-32.2	-60.3	———	0.0876	0.0034	———	-2.79
16	563.0	-30.2	-57.5	-76.0	0.1096	0.0047	0.0006	-2.44
17	563.5	-29.5	-55.6	-73.4	0.1189	0.0059	0.0008	-2.09
18	564.0	-30.8	-55.2	-74.0	0.1023	0.0062	0.0007	-1.74
19	564.5	-33.3	-55.5	-74.7	0.0772	0.0060	0.0007	-1.39
20	565.0	-35.5	-55.8	-71.8	0.0599	0.0058	0.0009	-1.04
21	565.5	-37.3	-58.0	-70.2	0.0484	0.0045	0.0011	-0.67
22	566.0	-38.9	-60.5	-71.4	0.0403	0.0033	0.0010	-0.34
23	566.5	-40.3	-61.5	-76.0	0.0345	0.0030	0.0006	0.00
24	567.0	-41.7	-61.7	-80.0	0.0293	0.0029	———	0.36
25	567.5	-42.5	-61.3	-81.3	0.0266	0.0031	———	0.71
26	568.0	-42.6	-60.8	-80.3	0.0263	0.0032	———	1.06
27	568.5	-43.1	-62.2	———	0.0250	0.0028	———	1.41
28	569.0	-43.3	-63.7	———	0.0243	0.0023	———	1.76
29	569.5	-43.8	-65.9	———	0.0230	0.0018	———	2.11
30	570.0	-44.5	-68.0	———	0.0213	0.0014	———	2.46
31	570.5	-45.2	-69.6	———	0.0196	0.0012	———	2.81
32	571.0	-45.6	-70.9	———	0.0186	0.0010	———	3.16
33	571.5	-46.2	-71.7	———	0.0174	0.0009	———	3.51
34	572.0	-46.8	-72.7	———	0.0162	———	———	3.86
35	572.5	-47.5	-73.3	———	0.0150	———	———	4.21
36	573.0	-47.5	-73.5	———	0.0150	———	———	4.56
37	573.5	-48.2	-77.0	———	0.0139	———	———	4.91

mode	time	f_u	f_L	f_r	Q	E
010	40	567.99	565.11	566.55	196.79	0
020	43	1128.94	1125.12	1127.03	295.42	-0.54×10^{-2}
030	46	1698.43	1693.67	1696.05	355.76	-0.21×10^{-2}
100	49	1129.10	1125.21	1127.15	289.76	0.11×10^{-3}

TABLE IV (Fig. 10)

mode	time	f_u	f_L	f_r	Q	E
010	0	566.19	563.20	564.70	189.30	0
020	3	1128.86	1124.95	1126.91	287.70	-0.2×10^{-2}
030	6	1696.18	1691.38	1693.78	353.24	-0.18×10^{-3}
100	9	1128.46	1124.62	1126.54	293.29	-0.32×10^{-3}

V_1=-11dB	time	f	V_2	V_3	V_4	P_2/P_1	P_3/P_1	P_4/P_1	FP
	12	558.7	-42.8	-69.8	———	0.0257	0.0011	———	-4.04
	13	559.2	-41.8	-68.7	———	0.0288	0.0013	———	-3.71
	14	559.7	-40.8	-67.9	———	0.0324	0.0014	———	-3.37
	15	560.2	-39.7	-66.9	———	0.0367	0.0016	———	-3.04
	16	560.7	-38.3	-65.5	———	0.0434	0.0019	———	-2.71
	17	561.2	-36.7	-63.5	———	0.0519	0.0024	———	-2.38
	18	561.7	-34.9	-61.0	———	0.0638	0.0032	———	-2.04
	19	562.2	-33.0	-57.8	-76.3	0.9794	0.0046	———	-1.71
	20	562.7	-30.7	-53.7	-70.7	0.1041	0.0074	0.0010	-1.38
	21	563.2	-28.9	-50.2	-65.3	0.1274	0.0110	0.0019	-1.04
	22	563.7	-28.5	-47.5	-61.4	0.1334	0.0150	0.0030	-0.71
	23	564.2	-30.4	047.2	-59.0	0.1078	0.0155	0.0040	-0.38
	24	564.7	-32.2	-48.5	-58.5	0.0873	0.0133	0.0042	-0.05
	25	565.2	-33.7	-52.2	-62.7	0.0733	0.0087	0.0026	0.29
	26	565.7	-35.6	-56.4	-70.07	0.0592	0.0054	0.0010	0.62
	27	566.2	-37.0	-58.4	-74.7	0.0501	0.0043	———	0.95
	28	566.7	-39.6	-59.7	-77.2	0.0314	0.0037	———	1.29
	29	567.2	-42.1	-61.5	———	0.0279	0.0030	———	1.62
	30	567.7	-43.7	-63.7	———	0.0232	0.0023	———	1.95
	31	568.2	-44.5	-65.5	———	0.0221	0.0019	———	2.29
	32	568.7	-45.1	-66.9	———	0.0197	0.0016	———	2.62
	33	569.2	-45.6	-68.0	———	0.0186	0.0014	———	2.95
	34	569.7	-46.1	-69.0	———	0.0176	0.0013	———	3.29
	35	570.2	-46.6	-69.8	———	0.0167	0.0012	———	3.62
	36	570.7	-47.0	-70.4	———	0.0158	0.0011	———	3.95
	37	571.2	-47.2	-70.6	———	0.0155	0.0011	———	4.28
	38	571.7	-47.7	-71.3	———	0.0146	0.0010	———	4.62
	39	572.2	-48.6	-63.9	———	0.0132	0.0023	———	4.95

mode	time	f_u	f_L	f_r	Q	E
010	42	566.35	563.33	564.84	186.79	0
020	45	1129.43	1125.52	1127.48	1287.84	-0.19×10^{-2}
030	48	1697.04	1692.26	1694.65	353.94	-0.78×10^{-4}
100	51	1129.12	1125.28	1127.20	294.16	-0.24×10^{-3}

TABLE V (Fig. 11)

mode	time	f_u	f_L	f_r	Q	E
010	0	566.90	563.86	565.38	185.80	0
020	3	1127.19	1123.28	1125.23	288.08	-0.49×10^{-2}
030	6	1695.31	1690.47	1692.89	349.27	-0.19×10^{-2}
100	9	1126.76	1122.90	1124.83	291.41	-0.36×10^{-3}

V_1=-11dB	time	f	V_2	V_3	V_4	P_2/P_1	P_3/P_1	P_4/P_1	FP
	12	559.4	-39.5	-66.9	———	0.0376	0.0016	------	-3.99
	13	559.9	-37.9	-65.3	———	0.045	0.0019	------	-3.66
	14	560.4	-36.4	-63.9	———	0.054	0.0023	------	-3.33
	15	560.9	-34.5	-61.8	———	0.0672	0.0029	------	-3.00
	16	561.4	-32.4	-59.1	-78.0	0.0856	0.0039	------	-2.66
	17	561.9	-30.3	-55.7	-72.7	0.109	0.0058	0.0008	-2.33
	18	562.4	-28.7	-55.6	-68.2	0.131	0.0059	0.0014	-2.00
	19	562.9	-28.9	-50.8	-65.3	0.127	0.0103	0.0017	-1.67
	20	563.4	-30.9	-50.0	-62.5	0.101	0.0112	0.0027	-1.34
	21	563.9	-32.3	-49.7	-60.3	0.081	0.0116	0.0034	-1.01
	22	564.4	-34.7	-50.9	-61.4	0.065	0.0101	0.0030	-0.67
	23	564.9	-36.3	-54.3	-67.0	0.055	0.0068	0.0016	-0.34
	24	565.4	-37.5	-59.3	-75.2	0.048	0.0038	------	-0.01
	25	565.9	-38.4	-65.0	———	0.043	0.0020	------	-0.32
	26	566.4	-39.3	-69.7	———	0.039	0.0012	------	-0.65
	27	566.9	-39.7	-72.2	———	0.037	0.0009	------	0.98
	28	567.4	-40.6	-74.5	———	0.033	------	------	1.32
	29	567.9	-40.7	-75.4	———	0.030	------	------	1.65
	30	568.4	-41.6	-73.5	———	0.030	------	------	1.98
	31	568.9	-44.0	-71.5	———	0.022	0.0009	------	2.31
	32	569.4	-47.3	-70.9	———	0.015	0.0010	------	2.64
	33	569.9	-49.1	-71.1	———	0.012	0.0010	------	2.97
	34	570.4	-49.9	-71.6	———	0.011	------	------	3.31
	35	570.9	-50.0	-71.8	———	0.011	------	------	3.64
	36	571.4	-50.3	-72.3	———	0.011	------	------	3.97
	37	571.9	-50.4	-72.4	———	0.011	------	------	4.30
	38	572.4	-50.4	-72.4	———	0.011	------	------	4.63
	39	572.9	-51.1	-71.6	———	0.010	------	------	4.96

mode	time	f_u	f_L	f_r	Q	E
010	42	566.95	563.96	565.46	189.24	0
020	45	1127.31	1123.40	1125.37	288.18	-0.49×10^{-2}
030	48	1695.54	1690.73	1093.14	351.57	-0.27×10^{-3}
100	51	1126.98	1123.12	1125.05	291.39	-0.27×10^{-3}

TABLE VI (Fig. 12)

mode	time	f_u	f_L	f_r	Q	E
010	0	564.94	562.04	563.49	194.44	0
020	3	1137.75	1133.55	1135.65	270.78	0.77×10^{-2}
030	6	1699.31	1694.34	1696.82	341.28	0.28×10^{-2}
100	9	1137.85	1133.56	1135.71	264.96	0.48×10^{-4}

V_1=-11dB	time	f	V_2	V_3	V_4	P_2/P_1	P_3/P_1	P_4/P_1	FP
	12	557.5	-53.7	-73.9	-76.2	0.0073	0.0007	———	-4.30
	13	558.0	-53.3	-74.2	-76.3	0.0077	———	———	-3.96
	14	558.5	-52.6	-74.6	-77.3	0.0083	———	———	-3.62
	15	559.0	-52.0	-75.1	-80.2	0.0089	———	———	-3.27
	16	559.5	-51.2	-85.3	-85.0	0.0098	———	———	-2.93
	17	560.0	-50.4	-75.3	———	0.0107	———	———	-2.58
	18	560.5	-49.6	-74.9	———	0.0117	———	———	-2.24
	19	561.0	-49.0	-73.3	———	0.0126	0.0008	———	-1.89
	20	561.5	-48.2	-71.6	———	0.0139	0.0009	———	-1.55
	21	562.0	-47.7	-69.7	———	0.0146	0.0012	———	-1.21
	22	562.5	-47.1	-67.2	———	0.0158	0.0015	———	-0.86
	23	563.0	-46.3	-64.7	———	0.0172	0.0021	———	-0.52
	24	563.5	-45.5	-61.3	———	0.0188	0.0031	———	-0.17
	25	564.0	-44.4	-58.1	———	0.0215	0.0044	———	0.17
	26	564.5	-42.7	-55.0	———	0.0260	0.0063	———	0.52
	27	565.0	-40.5	-52.7	———	0.0335	0.0082	———	0.86
	28	565.5	-38.8	-51.8	-56.5	0.0407	0.0092	———	1.21
	29	566.0	-37.0	-53.3	-67.5	0.0504	0.0077	0.0015	1.55
	30	566.5	-35.5	-55.5	-67.0	0.0596	0.0060	0.0016	1.89
	31	567.0	-34.1	-56.6	-67.5	0.0700	0.0052	0.0015	2.24
	32	567.5	-32.8	-56.9	-63.3	0.0813	0.0051	0.0024	2.58
	33	568.0	-32.3	-57.9	-60.3	0.0861	0.0045	0.0034	2.93
	34	568.5	-33.3	-61.3	-59.3	0.0072	0.0031	0.0038	3.27
	35	569.0	-35.4	-65.5	-60.0	0.0603	0.0019	0.0035	3.61
	36	569.5	-37.8	-67.0	-59.7	0.0457	0.0016	0.0037	3.96
	37	570.0	-40.2	-66.6	-60.0	0.0349	0.0017	0.0035	4.30
	38	570.5	-42.0	-66.2	-60.3	0.0282	0.0017	0.0034	4.65
	39	571.0	-43.6	-65.6	-60.5	0.0236	0.0019	0.0033	4.99
	40	571.5	-46.0	-68.6	-62.0	0.0178	0.0013	0.0028	5.34

mode	time	f_u	f_L	f_r	Q	E
010	43	565.47	562.56	564.01	193.75	0
020	46	1138.89	1134.67	1136.78	269.44	0.78×10^{-2}
030	49	1700.94	1695.60	1698.27	318.33	0.37×10^{-2}
100	52	1139.00	1134.76	1136.88	268.20	0.81×10^{-4}

TABLE VII (Fig. 13)

mode	time	f_u	f_L	f_r	Q	E
010	0	561.56	558.62	560.09	190.57	0
020	3	1137.45	1133.15	1135.30	264.33	0.14×10^{-1}
030	6	1694.09	1689.09	1691.59	338.39	0.67×10^{-2}
100	9	1137.58	1133.26	1135.42	263.01	0.11×10^{-3}

V_1=-11dB	time	f	V_2	V_3	V_4	P_2/P_1	P_3/P_1	P_4/P_1	FP
	12	554.1	-53.6	-74.7	———	0.0074	0.0007	———	-4.21
	13	554.6	-53.0	-74.7	———	0.0079	0.0007	———	-3.87
	14	555.1	-52.7	-74.7	———	0.0082	0.0007	———	-3.53
	15	555.6	-52.4	-75.5	———	0.0085	0.0006	———	-3.19
	16	556.1	-52.0	-76.1	———	0.0089	0.0006	———	-2.85
	17	556.6	-51.6	-76.7	———	0.0093	0.0005	———	-2.51
	18	557.1	-51.3	-77.5	———	0.0097	0.0005	———	-2.17
	19	557.6	-50.9	-77.5	———	0.0101	0.0005	———	-1.83
	20	558.1	-50.3	-76.9	———	0.0108	0.0005	———	-1.48
	21	558.6	-49.9	-75.1	———	0.0114	0.0006	———	-1.14
	22	559.1	-49.2	-72.8	———	0.0124	0.0008	———	-0.80
	23	559.6	-48.7	-70.3	———	0.0130	0.0011	———	-0.46
	24	560.1	-48.2	-67.5	———	0.0139	0.0015	———	-0.12
	25	560.6	-47.6	-65.0	———	0.0148	0.0020	———	0.22
	26	561.1	-47.0	-62.7	———	0.0158	0.0026	———	0.56
	27	561.6	-46.3	-60.4	———	0.0172	0.0034	———	0.90
	28	561.1	-45.4	-57.2	———	0.191	0.0049	———	1.24
	29	562.6	-44.5	-55.0	———	0.0211	0.0063	———	1.58
	30	563.1	-43.8	-54.4	———	0.0230	0.0068	———	1.92
	31	563.6	-43.1	-55.0	———	0.0248	0.0063	———	2.26
	32	564.1	-42.4	-57.5	———	0.0269	0.0047	———	2.61
	33	564.6	-41.2	-60.9	———	0.0309	0.0032	———	2.95
	34	565.1	-40.0	-64.5	———	0.0355	0.0021	———	3.29
	35	565.6	-38.6	-67.9	———	0.0417	0.0014	———	3.63
	36	566.1	-37.0	-70.6	———	0.0501	0.0010	———	3.97
	37	566.6	-35.2	-73.7	———	0.0617	0.0070	———	4.31
	38	567.1	-33.2	-71.0	———	0.0776	0.0010	———	4.65
	39	567.6	-31.5	-66.3	———	0.0944	0.0017	———	4.99

mode	time	f_u	f_L	f_r	Q	E
010	43	561.94	559.01	560.47	191.35	0
020	46	1138.34	1134.01	1136.18	261.97	0.14×10^{-1}
030	49	1695.35	1690.34	1692.85	338.37	0.68×10^{-2}
100	52	1138.44	1134.07	1136.25	260.07	0.69×10^{-4}

TABLE VIII (Fig. 14)

mode	time	f_u	f_L	f_r	Q	E
010	0	564.94	561.90	563.42	185.40	0
020	3	1137.18	1126.60	1128.89	246.64	0.18×10^{-2}
030	6	1703.17	1698.34	1700.75	352.63	0.62×10^{-2}
100	9	1139.73	1135.13	1137.43	247.16	0.76×10^{-2}

V_1=-11dB	time	f	V_2	V_3	V_4	P_2/P_1	P_3/P_1	P_4/P_1	FP
	12	557.5	-50.4	-74.2	———	0.0107	———	———	-3.92
	13	558.0	-50.0	-74.2	———	0.0112	———	———	-3.59
	14	558.5	-49.5	-74.2	———	0.0120	———	———	-3.26
	15	559.0	-48.9	-74.3	———	0.0127	———	———	-2.93
	16	559.5	-48.4	-74.5	———	0.0136	———	———	-2.59
	17	560.0	-47.7	-74.3	———	0.0147	———	———	-2.26
	18	560.5	-47.0	-73.9	———	0.0158	———	———	-1.93
	19	561.0	-46.3	-73.0	———	0.0172	———	———	-1.60
	20	561.5	-45.5	-71.1	———	0.0188	0.0010	———	-1.27
	21	562.0	-44.6	-68.5	———	0.0209	0.0013	———	-0.94
	22	562.5	-43.6	-65.3	———	0.0236	0.0019	———	-0.61
	23	563.0	-42.5	-62.1	———	0.0267	0.0028	———	-0.28
	24	563.5	-41.5	-59.3	———	0.0299	0.0039	———	0.05
	25	564.0	-40.6	-57.0	-76.0	0.0331	0.0050	———	0.38
	26	564.5	-40.0	-54.7	-71.8	0.0355	0.0065	0.0009	0.71
	27	565.0	-40.8	-54.0	-70.5	0.0324	0.0071	0.0011	1.04
	28	565.5	-42.0	-54.1	-71.3	0.0282	0.0070	0.0010	1.37
	29	566.0	-42.6	-54.7	-70.2	0.0265	0.0066	0.0011	1.70
	30	566.5	-41.2	-54.7	-64.8	0.0310	0.0065	0.0020	2.03
	31	567.0	-39.3	-55.3	-63.0	0.0387	0.0061	0.0025	2.36
	32	567.5	-37.0	-57.4	-67.2	0.0501	0.0048	0.0010	2.69
	33	568.0	-35.0	-58.7	-72.3	0.0631	0.0041	0.0009	3.02
	34	568.5	-33.0	-58.0	-75.5	0.0794	0.0045	———	3.35
	35	569.0	-32.6	-57.5	-79.0	0.0832	0.0047	———	3.68
	36	569.5	-33.6	-58.5	———	0.0741	0.0042	———	4.02
	37	570.0	-35.5	059.9	———	0.0596	0.0036	———	4.35
	38	570.5	-37.4	-63.5	———	0.0480	0.0024	———	4.68

mode	time	f_u	f_L	f_r	Q	E
010	0	564.94	561.93	563.43	187.00	0
020	3	1131.26	1126.70	1128.98	247.64	0.19×10^{-2}
030	6	1703.35	1698.48	1700.92	349.34	0.63×10^{-2}
100	9	1139.88	1135.27	1137.58	247.14	0.76×10^{-2}

TABLE VIII (Fig. 15)

mode	time	f_u	f_L	f_r	Q	E
010	0	561.20	558.27	559.73	190.78	0
020	3	1125.25	1120.66	1122.96	244.76	0.31×10^{-2}
030	6	1700.26	1695.60	1697.93	364.21	0.11×10^{-1}
100	9	1143.88	1139.80	1141.84	280.07	0.17×10^{-1}

V_1=-11dB	time	f	V_2	V_3	V_4	P_2/P_1	P_3/P_1	P_4/P_1	FP
	12	553.7	-52.7	-77.8	———	0.0082	0.0005	———	-4.17
	13	554.2	-52.4	-78.2	———	0.0086	———	———	-3.83
	14	554.7	-51.8	-78.2	———	0.0091	———	———	-3.49
	15	555.2	-51.4	-78.4	———	0.0095	———	———	-3.15
	16	555.7	-51.0	-79.0	———	0.0100	———	———	-2.81
	17	556.2	-50.5	-79.5	———	0.0107	———	———	-2.47
	18	556.7	-49.7	-79.7	———	0.0116	———	———	-2.13
	19	557.2	-49.1	-78.9	———	0.0124	———	———	-1.79
	20	558.2	-47.8	-75.7	———	0.0145	———	———	-1.12
	21	558.7	-47.0	-72.7	———	0.0158	———	———	-0.78
	22	559.2	-46.0	-70.0	———	0.0178	0.0011	———	-0.44
	23	559.7	-45.0	-67.3	———	0.0200	0.0015	———	-0.10
	24	560.2	-43.6	-65.3	———	0.0234	0.0019	———	0.24
	25	560.7	-42.6	-64.0	———	0.0264	0.0022	———	0.58
	26	561.2	-41.0	-61.7	———	0.0316	0.0029	———	0.92
	27	561.7	-40.5	-69.4	———	0.0335	0.0012	———	1.25
	28	562.2	-41.0	-68.5	———	0.0316	0.0013	———	1.59
	29	562.7	-43.2	-58.3	———	0.0247	0.0043	———	1.93
	30	563.2	-46.0	-58.8	———	0.0178	0.0041	———	2.27
	31	563.7	-49.0	-58.9	———	0.0126	0.0041	———	2.61
	32	564.2	-51.7	-57.9	———	0.0092	0.0045	———	2.95
	33	564.7	-53.6	-55.9	-69.0	0.0074	0.0057	0.0013	3.29
	34	565.2	-54.4	-53.9	-64.5	0.0068	0.0072	0.0021	3.63
	35	565.7	-53.7	-51.5	-62.4	0.0073	0.0094	0.0027	3.97
	36	566.2	-52.4	-50.0	-61.9	0.-085	0.0085	0.0029	4.30
	37	566.7	-50.6	-50.7	-60.1	0.0105	0.0105	0.0035	4.64
	38	567.2	-49.7	-67.8	-56.0	0.0116	0.0115	0.0056	4.98

mode	time	f_u	f_L	f_r	Q	E
010	41	561.45	558.48	559.96	188.60	0
020	44	1125.52	1120.92	1123.22	243.91	0.29×10^{-2}
030	47	1700.77	1696.08	1698.43	362.29	0.11×10^{-1}
100	50	1144.24	1140.17	1142.21	280.92	0.17×10^{-1}

BIBLIOGRAPHY

1. Coppens, A.B., and Sanders, J.V., "Finite-Amplitude Standing Waves in Rigid Walled Tubes," J. Acoust. Soc. AM., Vol. 43, pp. 516-529, Mar 1968.

2. Coppens, A.B., and Sanders, J.V., "Finite-Amplitude Waves Within Real Cavities," J. Acoust. Soc. AM., Vol. 58, pp. 1133-1140, Dec 1975.

3. Aydin, M., Theoretical Study of Finite-Amplitude Standing Waves in Rectangular Cavities With Perturbed Boundaries, Thesis, Naval Postgraduate School, Monterey, California, 1978.

4. Kuntsal, E., Finite Amplitude Standing Waves in Rectangular Cavities with Perturbed Boundaries, Thesis, Naval Postgraduate School, Monterey, California, 1978.

LIST OF REFERENCES

1. Coppens, A.B., Private Note.

2. Blackstock, D.T., J. Acoust. Soc. AM., Vol. 36, 217(L), 1964.

3. Fay, R.D., "Successful Methods of Attack on Progressive Finite Waves," J. Acoust. Soc AM., Vol. 26, pp. 253-254, 1954.

4. Keck, W., and Beyer, R.T., "Frequency Spectrum of Finite Amplitude Ultrasonic Waves in Liquids," Phy. Fluid, Vol. 3, pp. 346-352, 1960.

INITIAL DISTRIBUTION LIST

		No. Copies
1.	Defense Technical Information Center Cameron Station Alexandria, Virginia 22314	2
2.	Library, Code 0142 Naval Postgraduate School Monterey, California 93940	2
3.	Department Library, Code 61 Department of Physics and Chemistry Naval Postgraduate School Monterey, California 93940	2
4.	Professor James V. Sanders, Code 61Sd Department of Physics and Chemistry Naval Postgraduate School Monterey, California 93940	2
5.	Professor Alan B. Coppens, Code 61Cz Department of Physics and Chemistry Naval Postgraduate School Monterey, California 93940	1
6.	Dr. D. T. Blackstock Applied Research Laboratory University of Texas Austin, Texas 78712	1
7.	Library, Naval Academy Chin-Hae, Kyung Sang Nam Do KOREA	1
8.	Dr. Lee, C.H. Add, Chin-Hae, Kyung Sang Nam Do KOREA	1
9.	LT Ender Kuntgal Akatlar, Zeytinoglu Caddesl Satak Ap. 240/16 Etiler, Istanbul, TURKEY	1
10.	LT Mehmet Aydin Zincirlikuyu Caddesl No-99 Kasimpasa, Istanbul, TURKEY	1
11.	LTC Ilbok Joung Anti-Submarine Bureau Navy Headquarters, Seoul KOREA	6

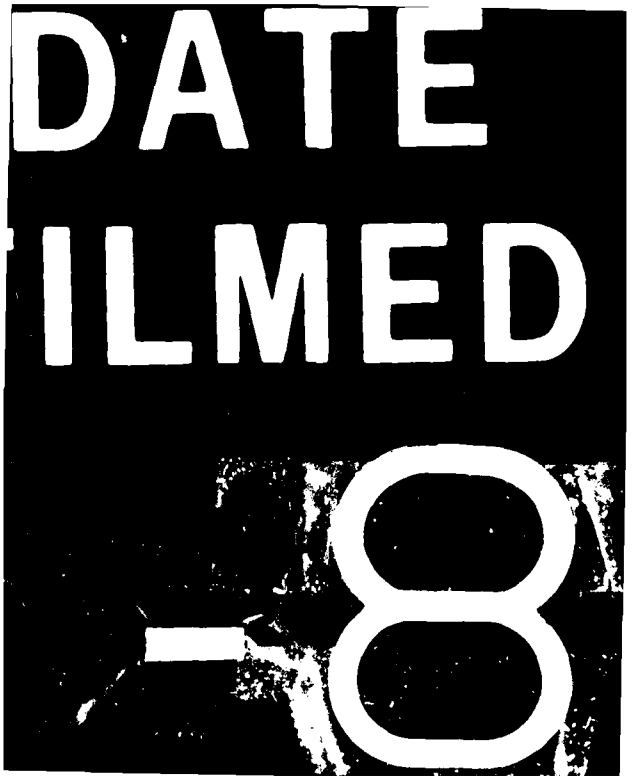
DATE
ILMED
-8